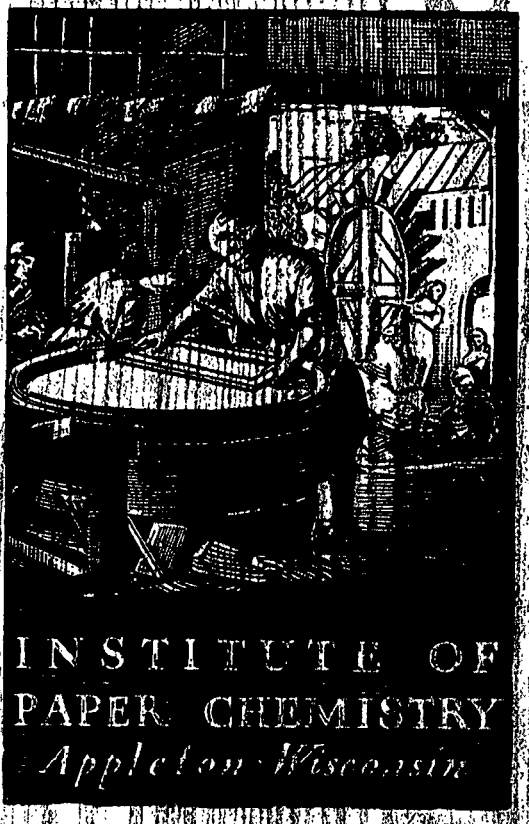

CORROSION RELATED FAILURES IN THE PULP AND PAPER INDUSTRY

Project 3309

Report One
A Progess Report
to
MEMBERS OF THE INSTITUTE OF PAPER CHEMISTRY

November 15, 1976

THE INSTITUTE OF PAPER CHEMISTRY

Appleton, Wisconsin

CORROSION RELATED FAILURES IN THE PULP AND PAPER INDUSTRY

Project 3309

Report One

A Progress Report

to

MEMBERS OF THE INSTITUTE OF PAPER CHEMISTRY

November 15, 1976

TABLE OF CONTENTS

THE INSTITUTE OF PAPER CHEMISTRY

Appleton, Wisconsin

CORROSION RELATED FAILURES IN THE PULP AND PAPER INDUSTRY

SUMMARY

Six corrosion failure analyses specific to the pulp and paper industry are presented in this report. Each problem was examined in terms of environmental factors, materials of construction, and the probable corrosion processes involved. Appropriate conclusions and recommendations were made in each instance.

The failure of kraft blow-tank target plates illustrated the rapid attack which can occur when corrosion is associated with erosion due to fluid impingement. The continuous removal of protective films accelerates electrochemical processes leading to rapid dissolution of metal. Although reduced jet impingement velocities should be helpful, greatest improvement is expected through the use of better target plate materials. Initial results in testing Illium PD stainless steel suggest its superiority in such service.

Severe corrosion of Type 304 stainless steel tubing in a kraft system wash liquor heater was attributed to chloride ion introduced during periodic cleaning with hydrochloric acid solutions. Pitting, stress corrosion cracking, and crevice corrosion were noted particularly in those areas where liquor flow velocities are low, drainage during shutdown is poor, and fibrous or other scale deposits are present. The problem can be minimized by water washing after acid cleaning, the use of safer cleaning solutions, or by the specification of tube materials better able to resist chloride ion attack.

Mild steel kraft white liquor pipelines failed rapidly in areas exposed to intense turbulence. Major corrosion problems were noted in areas where galvanic effects are expected due to coupling of the mild steel pipeline and stainless steel

components. Improved piping design to eliminate zones of intense turbulence and minimize galvanic action is indicated.

Mild steel steam generating tubes in a recovery boiler provided years of service in a kraft recovery operation. Serious fireside corrosion was encountered following a change from kraft to neutral sulfite semichemical operation. The presence of iron sulfide corrosion products pointed to sulfurous gases as the significant corrosive factor. The observed nonuniformity of corrosive attack was attributed to temperature and gas flow effects. Although the problem might be alleviated by employing alloy metal tubes, the preferred approach, adopted by the mill, involved a reduction in the sulfurous gas generation by reduced sulfidity of the NSSC liquor.

General corrosion of the mild steel collection hopper and corrosion fatigue failures of low-alloy rapper hammer assemblies in kraft recovery electrostatic precipitators was related to moisture condensation. The high rate of corrosion of the collection hopper was associated with poor seals permitting air entry, inadequate insulation and low gas temperatures. The maintenance of gas temperatures above the dew point is necessary throughout the entire system. The installation of thermocouples for temperature monitoring is recommended. The thread root failure of rapper bolts was identified as a corrosion fatigue problem which could be eliminated by stress reduction and the use of alloys or corrosion resistant plating.

The increased wear of corrugating rolls in recent years prompted an investigation into the possibility of combined wear and corrosion effects. The valleys of the flutes were free of the original chrome plate. The extreme wear in the flute valley and the flute tip appearance was characterized by severe

deformation and surface disruption generally describable as a perforated crater pattern. Surface fatigue was definitely indicated as a principal mechanism of wear in this roll. Corrosion, though possibly implicated, was not seen as a major cause of roll damage. Suggestions for the improvement of roll life include changes in roll construction and improved cleaning of the corrugated medium furnish to reduce the presence of hard contaminants.

INTRODUCTION

The success of a continuous operation as practiced in the pulp and paper industry depends upon uninterrupted production. Unexpected failures in production equipment are to be avoided. Perhaps the single most important factor in the design, installation and operation of this equipment is a well planned and executed preventative maintenance program. A necessary part of this program is corrosion control. Implementation of such a plan requires knowledge and application of the principles of corrosion technology. Losses due to corrosion can represent 20% of the total mill maintenance expenditure so that a sizeable return can be expected with suitable control techniques.

Basically, corrosive attack may appear in eight different forms and each form is indicative of the electrochemical activity occurring between the metal and its environment. The stability of the metal is determined by its ability to form a protective surface film which precludes continued oxidation or metal ion loss at the surface either by retarding penetration of harmful environmental species or slowing the outward diffusion of metal ions. This film must also have sufficient mechanical strength to withstand stress from applied loads and erosion from a flowing environment. If the film does not form or if it is weak and non-adherent, corrosive attack takes the form of uniform metal loss over large areas. Such corrosion is classified as general or uniform attack, erosion-corrosion, or selective leaching. When the surface film is adherent but allows ionic diffusion, corrosion appears as metal loss in localized regions. The forms of localized corrosion are pitting, crevice, galvanic and intergranular. The eighth form of corrosion results from a synergistic action of stress and corrosion, viz., stress corrosion cracking or corrosion fatigue. Operative mechanisms involved in each form of corrosion are primarily electrochemical in nature.

The form of corrosive attack is not only influenced by the prevailing conditions of the metal-environment couple but also by auxiliary processes of cleaning, lubrication, and repair. Acid cleaning, air and steam blowdown, caustic and/or water boilouts, steam and water impingement and mechanical brushing are common cleaning methods used in various systems throughout the mill. While the purpose of such treatments is to improve operating efficiency, in many cases these methods are the cause of severe corrosion damage and catastropic failure of the equipment. Inadequate lubrication or the use of improper lubricants accelerates corrosion and leads to premature equipment service life. Repairs can promote corrosive processes when these result in unfavorable metal couples or in the creation of notches, crevices, localized heating and high stresses.

In an effort to identify specific corrosion problems in our industry, a number of failure analyses have been performed on various items supplied by different mills. It is the purpose of this report to describe the results of these analyses. Failure analysis includes a review of the operating history, material and environmental properties, identification of the form(s) of corrosion associated with failure, and the possible causes and solution to the problem.

BLOW-TANK TARGET PLATES

The distribution systems which handle pulp-liquor slurries from the digester are subject to erosion-corrosion. Blow line piping, pumps, valves, blow pit or tank liners are common items which require routine replacement. The materials of construction in these applications range from mild steel to various types of stainless steel.

In the failure analysis which follows, a blow tank is used to collect the pulp and liquor discharge from several batch-type digesters. The blow tank shell is protected with liner plates. Two of these plates serve as a target to receive the main impact of the discharge. The 5/8-inch thick target plates are approximately 3 feet wide by 5 feet long. The plates are formed to a 71-1/2 inch outside radius to fit the tank circumference. The blow tank nozzle directs the incoming stream tangentially into the tank at a distance of 3 to 4 feet from the target plates. Figure 1 is a sketch of this system.

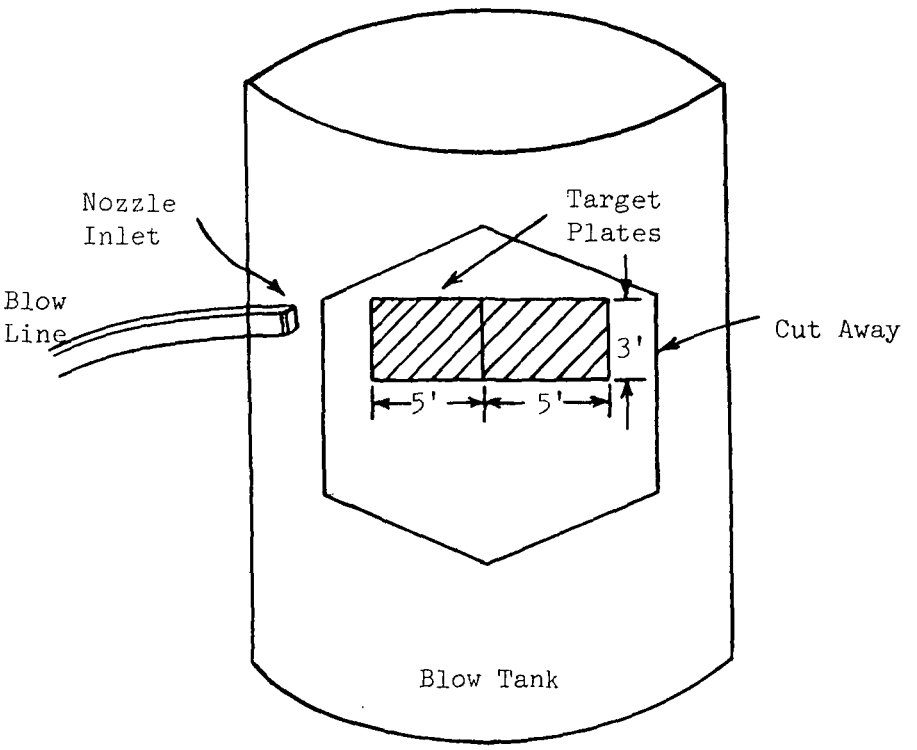

Figure 1. Sketch Showing Location of Target Plates in the Blow Tank with Respect to Blow Tank Inlet Nozzle

The target plate material is Firmex Orange*, a high strength, low alloy steel commonly used in equipment which must withstand both shock and wear in service. The chemical composition, Table I, shows a high percentage of manganese with somewhat lesser amounts of nickel and copper. These elements together with the boron and molybdenum additives enhance hardenability during heat treatment while vanadium and aluminum serve as grain refiners. The hardness and other mechanical properties indicate that the steel is heat treated in such a way as to provide maximum toughness with some sacrifice of abrasion resistance.

TABLE I

COMPOSITION AND MECHANICAL PROPERTIES OF FIRMEX ORANGE[a]

Element	Chemistry (wt. %) Specified	Chemistry (wt. %) Analyzed at IPC	Mechanical Properties (Specified)	
C	0.24-0.29	NA[b]		
Mn	1.8 -2.4	2.4	Tensile strength	165 ksi
B	0.005	NA	Yield strength	135 ksi
Si	0.15-0.30	0.30	% Elongation	18%
Mo	0.15-0.30	0.22	Bend	3T to 1
Ni	0.7 -1.0	NA	Hardness	280-325 BHN
Cu	0.15-0.50	0.40		
V	0.01-0.05			
Al	0.05-0.1			
P & S	0.35 Max			

[a]Trade name — International Alloy Steel Co.
[b]Not analyzed.

*Trade name — International Alloy Steel Company.

The properties of the black liquor and cooked chips blown from the digester are variable. These depend on the wood species, chip processing and cooking conditions. In addition, contaminants in the form of metal, rocks, sand, etc., can be a part of the process stream. Some representative properties of this environment are shown in Table II. The high temperature, pressure, and velocity are of particular importance in these data. The black liquor composition represents an analysis of liquor obtained at some later time in processing.

TABLE II

BLACK LIQUOR PROPERTIES

Black Liquor Composition

Concentration, g/l (as Na_2O)		Physical Properties	
Na_2O	44.4	Specific Gravity	1.27
NaOH	21.2	Viscosity	44 CPS
Na_2S	16.1	Boiling point increase	18.9°F
Na_2CO_3	55.1	pH	12 (based on 10 g/l alkali)
Total Na	153.2		
Combined Na	53.8	Organics/inorganics	68.9 / 31.1

Blow pressure — 140 psi

Temperature — 350°F

Calculated stream velocity — 21.1 ft/sec

FAILURE ANALYSIS

The target plates which receive the main impact of the pulp-liquor stream blown from the digester into the blow tank are particularly subject to rapid erosion-corrosion attack. The following analysis of blow-tank target failure is

of direct interest in this application. The results, however, are more generally applicable to all erosion-corrosion problems in kraft pulping liquor environments.

A photograph of a portion of the primary target plate which failed after 7.5 months service is shown in Fig. 2. This portion was cut from that part of the plate in nearest direct line with the blow tank nozzle. The complete loss of metal at the center and deep gouge marks surrounding it show the main impact area and the direction of flow after impingement. Small pits are located within each gouge mark where grains of metal have literally eroded away. Such deep spongy pitting is often associated with cavitation damage. Small cavities of vapor formed in the black liquor under high pressure during the blow cause an implosion as they collapse with return to normal pressure inside the blow tank. The implosion of cavities next to the target plate surface causes local work-hardening of the metal — these areas roughen and crack by fatigue.

Metal properties which confer protection against erosion-corrosion and cavitation are still a subject of controversy. Various studies have been conducted in an effort to reveal some of the important mechanisms involved in this attack (1-5). Others have characterized the appearance of high velocity jets and the damage sustained on target plates constructed of unconventional materials; e.g., pure Ni, Al single crystals, etc. (6). To date, there has been no direct correlation between material properties and its erosion-corrosion resistance.

Performance tests in erosion-corrosion environments using commercial metals and alloys have shown the major attack as a continuous local breakdown and removal of protective surface films from the metal by the impinging jet stream (7-8). When protective films are removed, the exposed metal becomes anodic to adjacent filmed areas and suffers rapid corrosion. The impinging solution depolarizes

cathode areas adjacent to the anodes thus enhancing electrochemical dissolution. The metal must withstand the mechanical forces and then possess sufficient protective film strength to resist breakdown by chemical attack.

Figure 2. Photograph of the Central Portion of the Primary Target Plate Showing Severe Erosion-Corrosion Damage

No corrosion data are given for Firmex Orange in any environment. Generally, low alloy steel is somewhat better in corrosion resistance than mild steel (9). However, iron or low-alloy iron based metals do not form protective surface films in high pH environments and rapidly erode away under the scouring action of flowing media. This deficiency also leads to poor resistance to cavitation and corrosion fatigue.

RECOMMENDATIONS

Perhaps the most effective way to combat erosion-corrosion problems is by changing the design of the system. The installation of screens and magnetic separators to help remove unwanted foreign matter from the chips is most desirable. The jet impingement velocity could be reduced by a larger blow line pipe, reduced pressure and/or increased nozzle area provided these changes comply with the necessary mechanical action imparted to the chips upon impact.

A change in target plate material is definitely indicated for this application. Suitable candidate materials would be the precipitation hardened stainless steels, Stellite alloy 6B or a wrought grade of stainless steel comparable to cast CD4MCu* or Illuim PD**. Consideration of cost, ease of fabrication and installation as well as expected service life prompted trial tests of the Illuim PD material. Cast test coupons of this material were installed in the secondary target plate area of the blow tank. After two months exposure, there was little, if any, metal loss. The composition and properties of Illuim PD are shown in Table III. This material has performed quite well in pumps and valves subjected to erosion-corrosion by pulp and liquor slurries. It is only available in the cast form. In view of its potential use for these applications throughout the industry, negotiations are currently underway with the supplier to provide a wrought form of this alloy.

* Alloy Casting Institute designation.
**Trade name — Stainless Foundry & Engineering, Inc.

TABLE III

COMPOSITION AND MECHANICAL PROPERTIES OF ILLUIM PD

Composition

C – 0.08	Mo – 2.0
Ni – 5.0	Co – 7.0
Cr – 27.0	Fe – Bal.

Mechanical Properties

Ultimate tensile strength (ksi)	– 115-125
Yield strength (ksi)	– 80-95
Elongation (%)	– 28-36
Hardness (BHN)	– 255-269

WHITE LIQUOR PIPELINE

Uninterrupted supply of liquors, bleaches, aqueous chemical media and all types of water rely on the integrity of miles of pipelines. In the kraft process, make-up (white and green) liquors as well as cooking or spent (black) liquors are often handled in mild steel pipelines. The internal pipe surface is subjected to corrosive attack by the highly alkaline, flowing media in these applications.

In the case history which follows, a mild steel pipeline was used to conduct white liquor from the causticizer to the filter. The Schedule 40 pipe sections consisted of the following: a 10 inch I.D. pipe descending 30 feet from the causticizer to a catch basin at the pump station, the 10 inch I.D. by 6 feet long catch basin with two reduced sections for pump intakes, one operating and one spare Type 316 stainless steel pumps, and a 4 inch I.D. pipe from the pumps to the white liquor filter. The causticizer tank was constructed of Type 304L stainless steel and the slaker is lined with Type 304 while its moving parts are Type 316 stainless steel. The chemical composition of all materials is given in Table IV. The pipeline was installed by welding at the required locations.

TABLE IV

CHEMICAL COMPOSITION OF PIPELINE
MATERIAL AND RELATED EQUIPMENT

	Content (wt.%)						
Item	C	Mn	P	S	Ni	Cr	Mo
Pipe	0.25	0.95	0.05	0.06	--	--	--
Pump	0.08	2.0	0.04	0.03	10-14	16-18	2-3
Tank	0.03	2.0	0.04	0.03	8-12	18-20	--
Slaker	0.08	2.0	0.04	0.03	8-12	18-20	--

The white liquor slurry composition varies because of changes in the effectiveness in slaking and causticizing operations. A typical slurry analysis and liquor flow rate is shown in Table V. Liquor temperature is approximately 100°C and the pH is quite high.

TABLE V

WHITE LIQUOR SLURRY COMPOSITION AND FLOW RATE

Solids content – 15%

White liquor analysis:

Sodium hydroxide	53.3%
Sodium carbonate	23.0%
Sodium sulfide	23.6%
Chloride content	0.35%

Velocity of Slurry	Nominal Flow 280 gpm	Maximum Flow 400 gpm
10 inch pipe	1.14 ft./sec	1.63 ft./sec
6 inch pipe	3.11 ft./sec	4.44 ft./sec
4 inch pipe	7.06 ft./sec	10.1 ft./sec

FAILURE ANALYSIS

The white liquor line operated only 3 months before leaks developed in the catch basin adjacent to the pump station. The photograph in Fig. 3 shows three locations marked by an "X," where failure occurred. It is seen that each location is on the top side of the pipe and just behind or adjacent to the points where various sections were welded in the main body. In addition, there is a spot marked A (left side of the photograph) adjacent to the flush line pipe. No failure occurred at this point. Each of these sections was cut from the main body for further investigation.

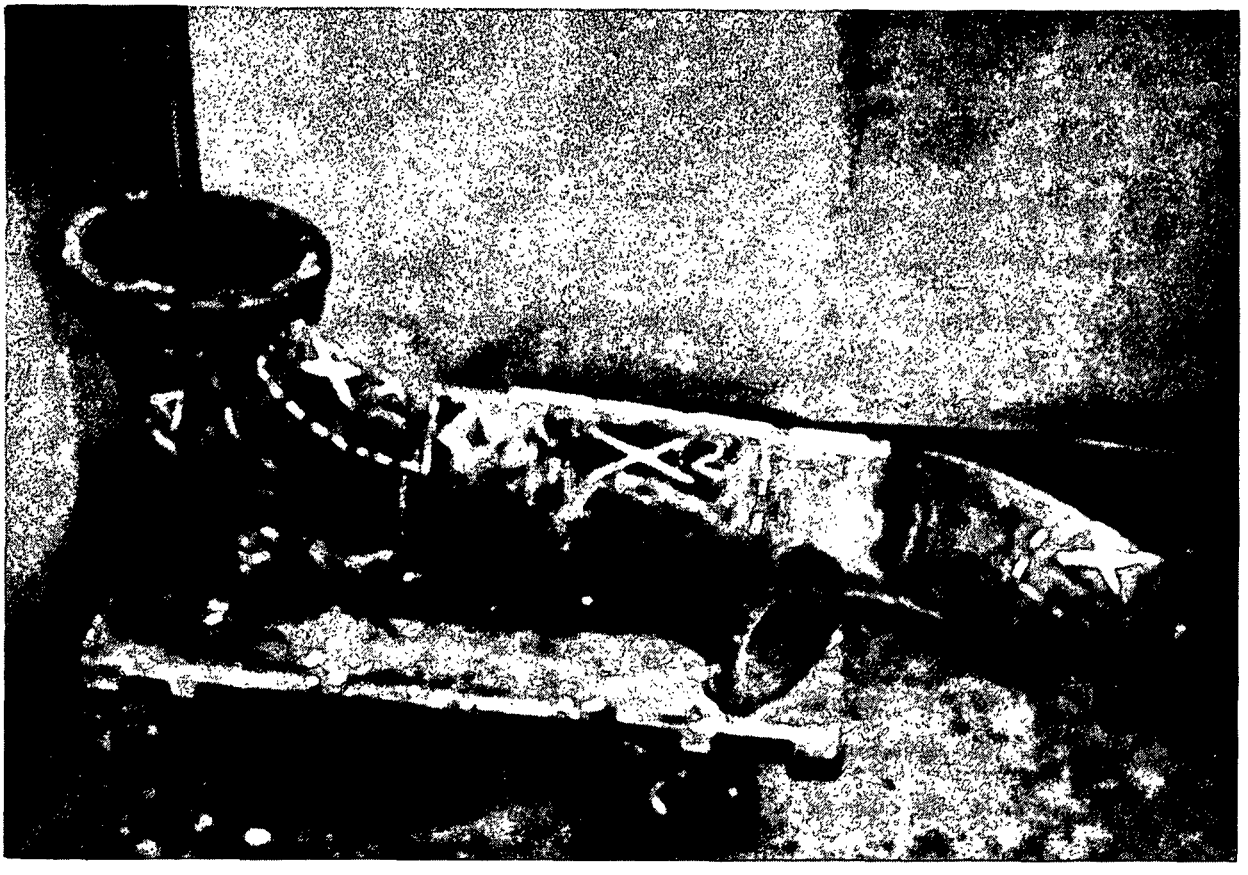

Figure 3. Photograph of Failed Section Showing the Relative Position of the Pipe in Service and its Overall Size. The X Marks Indicate the Location of Failure While the A Mark is a Location of Special Interest

An overall inspection of the pipe did not reveal any excessive corrosion attack except at the locations mentioned above. In fact, except where heavy encrustations existed at pump inlet points the pipe body was uniformly covered with a clean rust scale. Shallow channels or grooves were noted within the weld metal wherever joints were located. These grooves were distributed quite uniformly in the weld seam completely around the pipe circumference.

The photograph in Fig. 4 shows the inside of the pipe at location A. This picture is a typical appearance of erosion-corrosion. Note the "hills and valleys" and grooving that occurred in the center of this section. The entire spot (surrounded in white) is quite smooth and the grooves inside it are easily detected by feel. Although the pipe did not fail in this region, it would have done so with longer service times. The location of this attack is where erosion would be expected, i.e., near the bottom of the bend, but it undoubtedly was intensified by the flush line installation. The flush line extended beyond the inside diameter of the main pipe and aided the erosion in that area by creating additional turbulence.

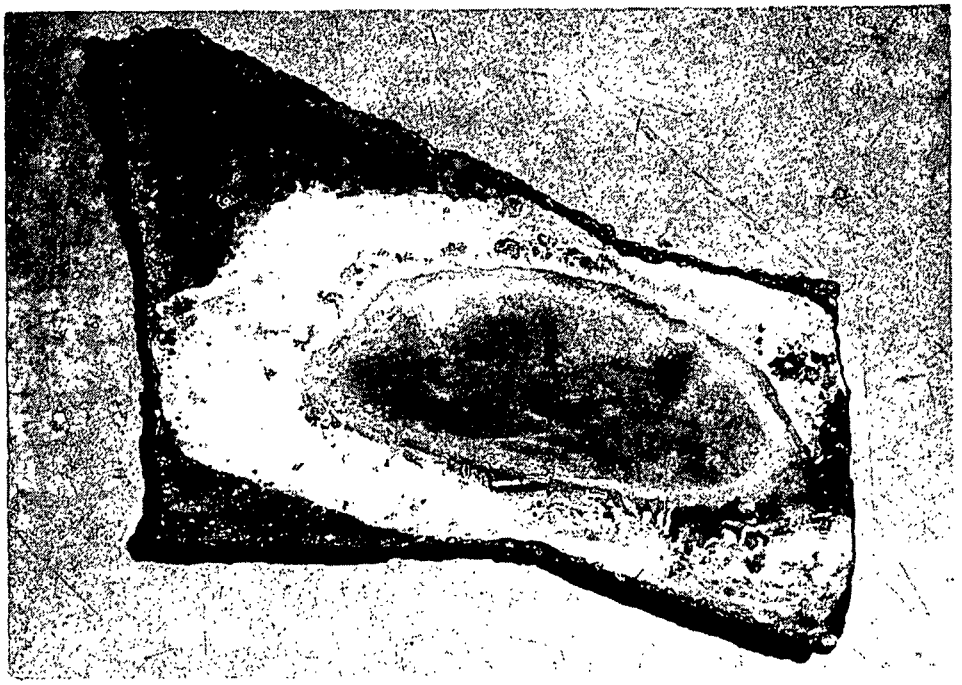

Figure 4. Photograph of Section Marked A in Figure 3. It Shows an Area of Erosion-Corrosion as Outlined by the White Lime Deposit

The photograph in Fig. 5 shows the inside surface of the pipe section cut from the top of the bend just below the 10-inch flanged end (left side of photo in Fig. 3). The large hole and remnants of the original metal seen to the right and center of the photograph demonstrates an area of extreme concentrated attack.

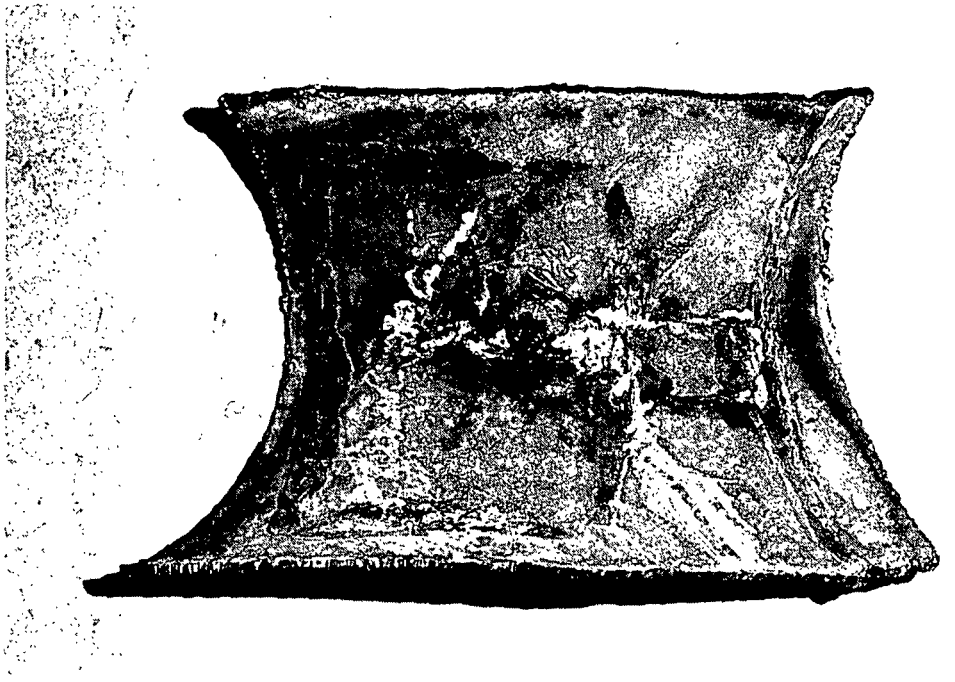

Figure 5. Photograph of the Pipe's Inside Surface at the Point of Failure Located at the Top of the Bend (Left Side of Figure 3).

The photograph in Fig. 6 and 7 show the inside surface of the pipe located at the two reduced sections. The pattern of corrosive attack is similar in these failure regions to that noted at the top of the bend.

Figure 6. Photograph of the Section Cut from the Failure Location at the Reduced Pipe Section (Center of Figure 3)

Definite attack in the form of channels and grooves was observed in all weld seams. An analysis of metal samples taken from these areas is shown in Table VI.

Figure 7. Photograph of the Section Cut from the Failure Located at the Other Reduced Section (Right X Mark in Figure 3)

TABLE VI

CHEMICAL COMPOSITION OF PIPE AND WELD

Element (wt.%)	Parent (Pipe)	Weld
Mn	1.10	0.62
Si	0.30	0.18
Al	0.28	0.0084
Cu	0.032	0.035
Others	N.D.[a]	N.D.
Fe (by comparison)	98.5	99.2

[a] None detected.

CONCLUSIONS

The major areas of failure are related to the hydraulic flow patterns at critical changes in section geometry (weld joints and reduced sections). The turbulence created at these locations was sufficient to remove films on the steel surface which would have offered some protection. Further enhancement of corrosion is attained by the high temperature, pH, and oxygen content of this environment.

It is likely that the corrosion rate at all three failure points was also increased by galvanic effects. In this case the mild steel anode area is small in size compared to the rather large stainless steel cathode area; e.g., causticizer tank, pumps, and slaker. Galvanic effects are always greatest under these conditions, i.e., small anode — large cathode (10). It is poor practice to couple an anodic material such as carbon steel to a large cathode of stainless steel with exposure to a nonpassivating electrolyte (11).

There were also areas in the pipe where erosion-corrosion processes could have caused failure with longer service time. The grooves and channels in the weld metal were also caused by this action. No metallurgical inconsistencies were indicated by the analysis of weld and parent metal. In this case, the solids contained in the slurry were abrasive enough to wear the mild steel surface at bend locations or weld metal obstructions.

RECOMMENDATIONS

1. Insofar as possible a change in pipe material from mild steel to Type 316L stainless steel is recommended. The protective surface film on the 316L alloy is stronger and it resists erosion, cavitation, and oxidation much better than mild steel for this application. Greater weld integrity is made possible by

the low carbon content in this alloy. This will help prevent sensitization, intergranular corrosion and weld zone attack. All junctions between mild steel and stainless steel construction must be insulated to eliminate the galvanic effects in the old system.

2. Pumps and valves should be adjusted so that the catch basin is kept full and flow distribution is more uniform. This will reduce the turbulence and the problems associated with it.

3. The pipeline should be thoroughly flushed out prior to any prolonged shutdown. Any deposits or encrustations resulting from solids settling out during the shutdown could cause crevice and pitting attack on the stainless steel surface beneath that deposit. This is particularly important in view of the relatively high chloride content in the white liquor (Table V).

LIQUOR HEATER TUBES IN KAMYR DIGESTER SYSTEM

Heat exchangers are employed to provide proper liquor and wash water temperatures in Kamyr digester. The primary liquor heaters are exposed to steam on the shell side and cooking liquor on the tube side. Kamyr wash liquor heater tubes are supplied with wash liquor from the first stage vacuum diffusion washers while the shell side is exposed to black liquor from the final pulping sections of the digester. The major operating problem with these heaters is poor heat transfer caused by deposition of scales and sediments from the liquors. Heat transfer is restored by removal of these deposits with acid cleaners. Corrosion problems are associated with both scale deposition and the cleaning of the heaters.

In the failure analysis which follows, the tube bundle in a wash liquor heater failed after two months operation. Both shell and tube construction material was Type 304 stainless steel. The tube bundle consists of 320 openings, one inch O.D. x 18 BWG (average welded wall) tubes (160 U-bends). The tubes were manufactured as prescribed by ASTMA-249. All internal baffles and tube supports are Type 304 stainless steel. Assembly was accomplished by welding in accordance with ASME — Unfired Pressure Vessel Code Section VIII.

The operating data for both primary and wash liquor heaters are given in Table VII. A relatively high chloride content is indicated in the liquors and the water. In addition, the heaters are periodically cleaned with inhibited hydrochloric acid.

FAILURE ANALYSIS

Samples from the U-bend and straight section of the wash liquor heater tubes are shown as received in Fig. 8. Visual inspection shows locations of severe attack as identified on the photograph by letter or number. Location 1 contains

TABLE VII

OPERATING DATA FOR KAMYR LIQUOR HEATERS

Upper and Lower Primary Heaters

	Tube Side (Liquor)	Shell Side (Steam)
Flow rate:	2000-2500 gpm	300-350 lb/min
Temperature:	320-340°F	365°F
Composition:	Solids 10-15%	
	pH 12.7	
	NaOH 16 g/liter	
	Na_2S 16 g/liter	
	CL 2400 ppm	
	Sp. Gr. 1.10	
Pressure:	300 psi	150 psi

Wash Liquor Heater

	Tube Side (Wash Liquor)	Shell Side (Black Liquor)
Flow rate:	400-600 gpm	1000-1160 gpm
Temperature:	Inlet (100°F)	Inlet (290-310°F)
	Outlet (280°F)	Outlet (260-280°F)
Composition:	Solids 2-3%	10-13%
	pH 10-11	12-13
	NaOH[a] 0.02 to 0.08	0.1 to 0.4
	Na_2S[a] 0.02 to 0.06	0.3 to 0.6
	Na_2CO_3 Present (amount not determined)	Present

Chloride — Chloride Content of Liquor and Water Supply

Item	Chloride Content (ppm)
White liquor	28.6-34.6
Artesian well water	2000
On-site well water	20-200
Treated river water	7000-9000

[a] Expressed in lb/ft^3 as Na_2O.

large corrosion pits and stress corrosion cracks while 2 and 3 show tears and cracks between pits distributed more toward the outside of the bend. Random pitting and crevice attack are present in Location 5 and 6. The straight section contains stress corrosion cracks at A and random pitting at B. All of these locations were examined more closely by sectioning the tubes at appropriate points.

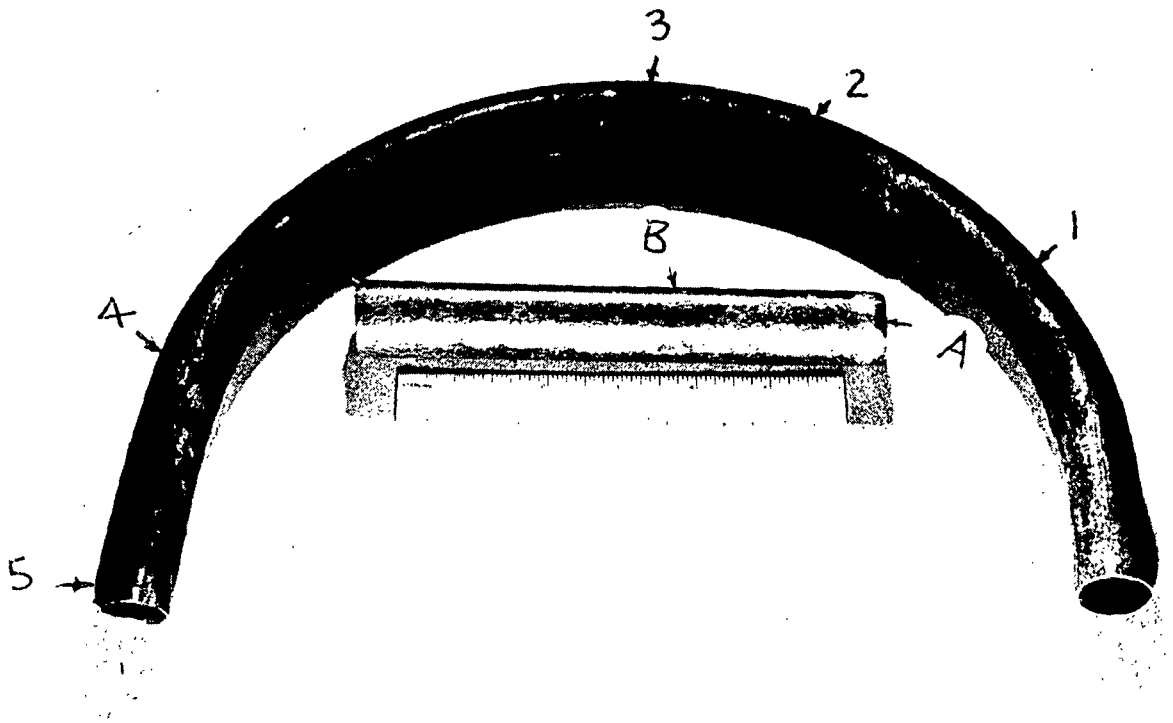

Figure 8. As Received Samples of Wash Liquor Heater Tube. Locations of Severe Corrosion Attack are Indicated by Numbers on the U-bend Section and Letters on the Straight Section

Pitting appears both on the outside and inside surfaces of the U-bend section but it is not as severe (as deep) on the outside surfaces — mainly associated with areas of heavy black stain. The more severe pitting on the inside

of the tube is beneath fibrous-scale deposits. In both cases the frequency of pitting is greatest on the outside of the bend. Figure 9 shows Locations 2 and 3 where this attack and fibrous deposits are clearly evident.

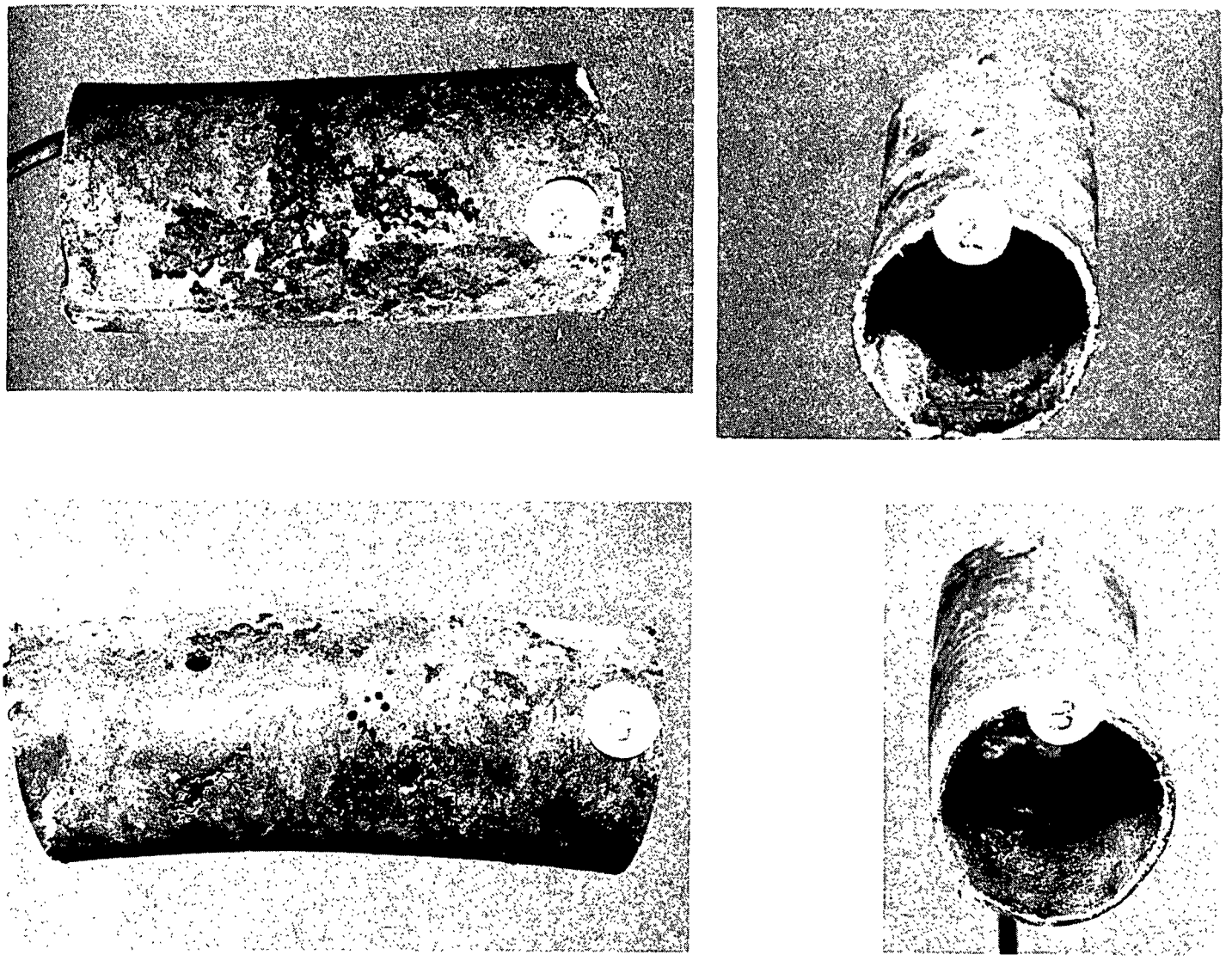

Figure 9. Top, Left — Pitting and Stress Corrosion Cracking Between Pits at Location 2 (Figure 8)
Top, Right — Fibrous Deposits Inside Tube at Location 2 (Figure 8)
Bottom, Left — Severe Pitting at Location 3 (Figure 8)
Bottom, Right — Fibrous Deposits Inside of Tube at Location 3 (Figure 8)

Stress corrosion cracking appears in a similar manner; i.e., frequency and severity is greatest on the outside of the bend where heavy fibrous deposits are present. Figure 10 shows this attack at Location 1. In this case the crack is seen emanating from a pit. Figure 11 shows another example of stress corrosion cracks and pitting in the straight tube section at Locations A and B.

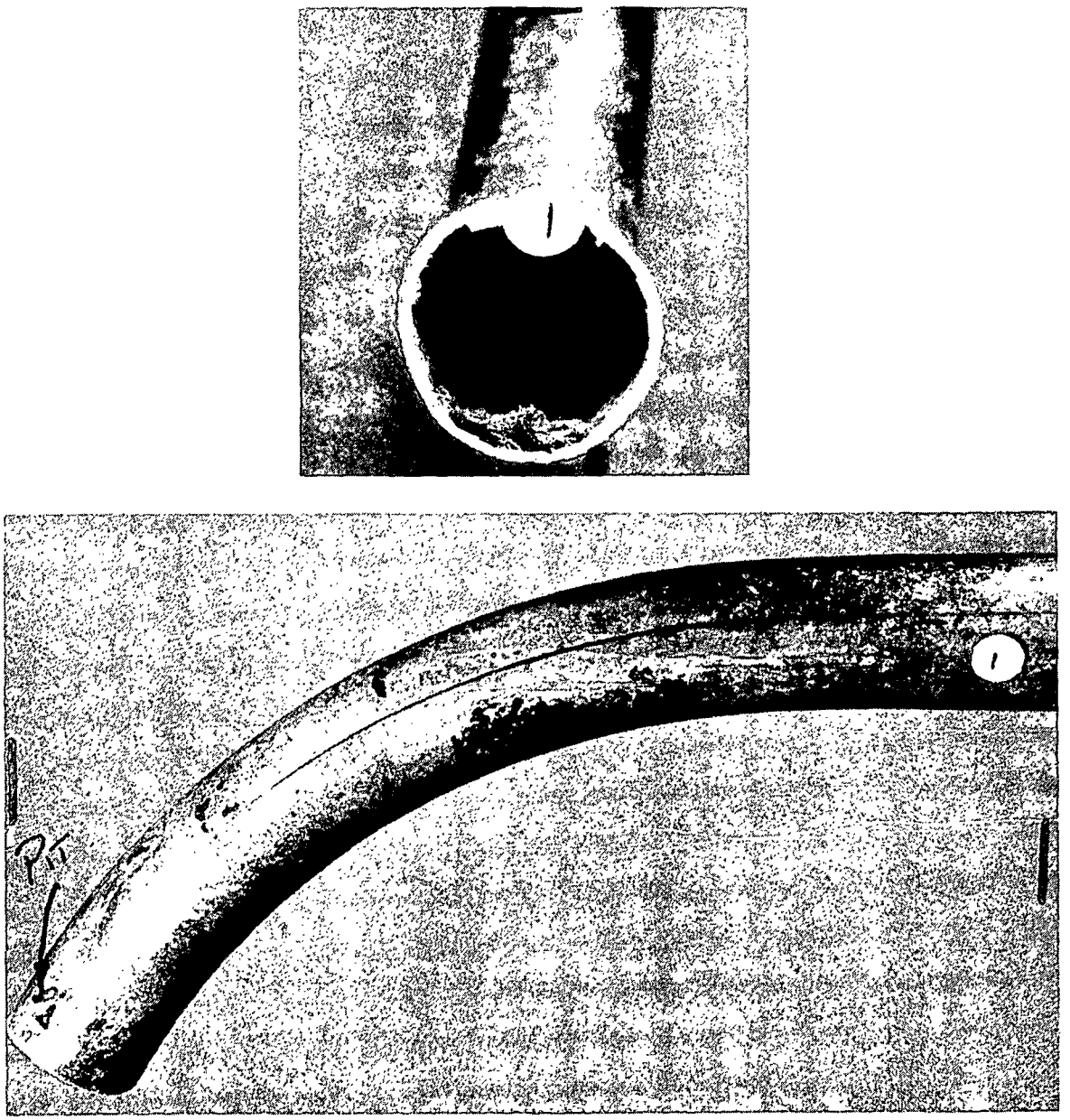

Figure 10. Bottom — Stress Corrosion Crack Emanating from a Pit at Location 1 (Figure 8)
Top — Heavy Fibrous Deposit on Inside of Tube at Location 1 (Pit End

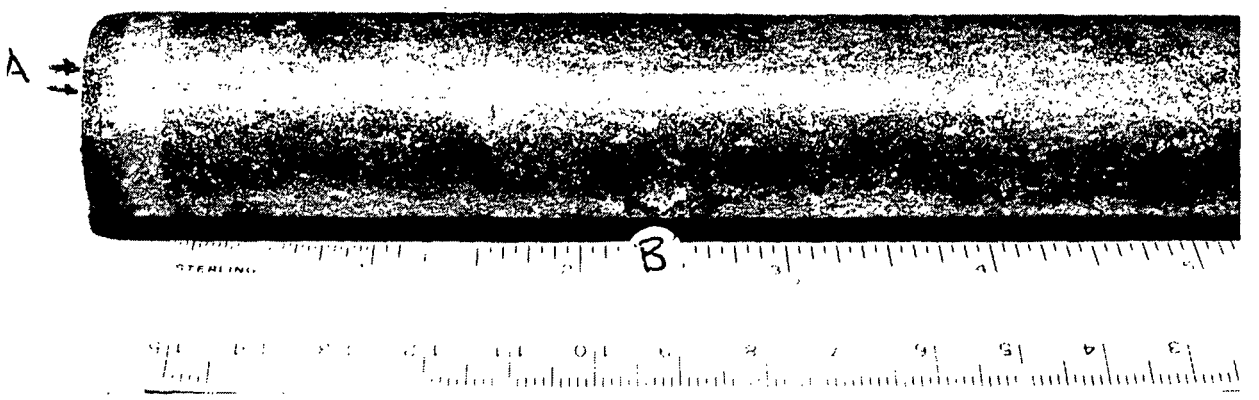

Figure 11. Close-up Photograph of Stress Corrosion Cracking and Pitting at Locations A and B, Respectively, in the Straight Section of Tube (Figure 8)

Samples of the fibrous deposit inside the tube, corrosion products on the outside as well as metal drillings from the severely corroded areas were analyzed for chloride content. Clean metal drillings were also obtained for carbon analysis. The results are shown in Table VIII.

Metallographic samples were taken from Location 1 to analyze the morphology of pitting and stress corrosion cracking and the grain structure in weld, parent metal, and heat affected metal zones. Figure 12 shows transgranular stress corrosion cracking at all pit locations while Fig. 13 shows the weld and heat affected zones (left) as a somewhat finer grain structure than that of the parent metal (right).

TABLE VIII

CHEMICAL ANALYSIS OF WASH LIQUOR TUBES

Chloride Determinations

Location	Composition wt.%	ppm
Outside of tube (metal drillings from corroded area)	0.38	3800
Outside of tube (filings from black liquor stain)	0.06	660
Inside of tube (fibrous deposits)	11.4	114,000

Metal Specification and Analysis (wt.%)

	ASTM A-249 TP 304	Tube Analysis
C	0.08 Maximum	0.07
Mn	2.0	
P	0.04	
S	0.03	
Si	0.75	
Ni	8.0 to 11.0	
Cr	18.0 to 20.0	
Mo	--	

The results in Table VIII show that a high concentration of chloride was present on the tube side of the heater. These results were obtained from the fibrous deposits inside the tube. It is also possible that chlorides were somewhat high on the shell side but the analyses from the outside of the tube could have been the result of leakage from the inside. The carbon content of the metal complies with the chemical composition specified by ASTM A-249.

The pitting and transgranular stress corrosion cracking depicted in Fig. 12 is typical of chloride attack in its two most prevalent corrosion forms on Type 304 stainless steel (12). There was no evidence of carbide precipitation or intergranular attack in the weld or heat affected zone. In addition, Fig. 13 shows that pitting attack was less severe on the outside of the tube, being confined to shallow penetrations at the grain boundaries. The lack of carbide

precipitation and the refined grain structure in the weld indicates that final heat treatment was correct as specified.

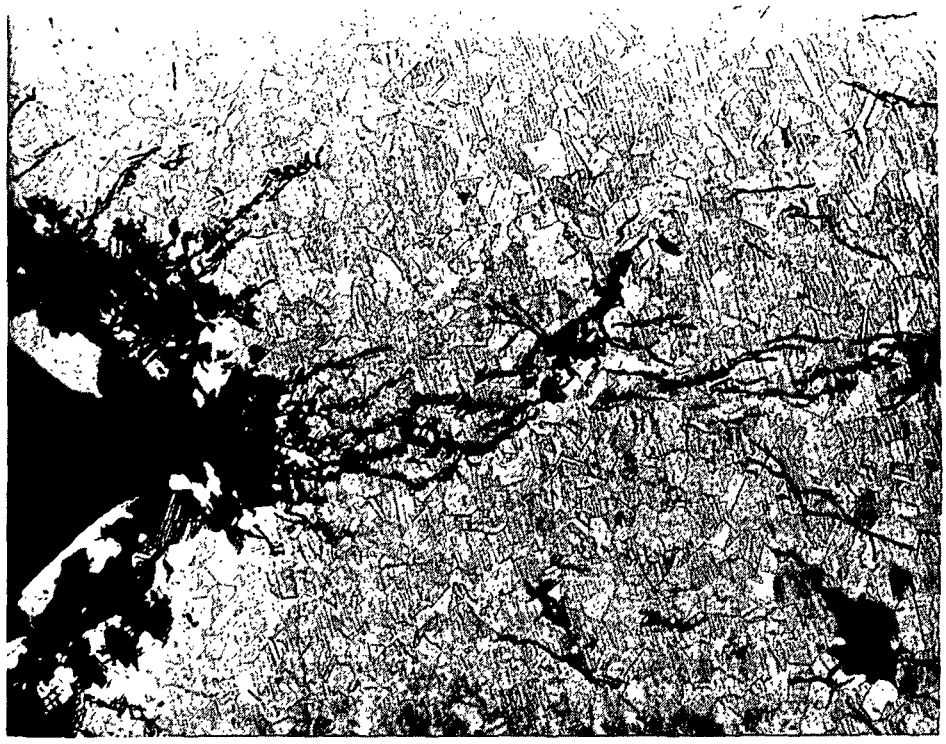

Figure 12. Transgranular and Branching Stress Corrosion Cracking Emanating from the Pit (Left Side of Photograph) at Location 1 (Figure 8)

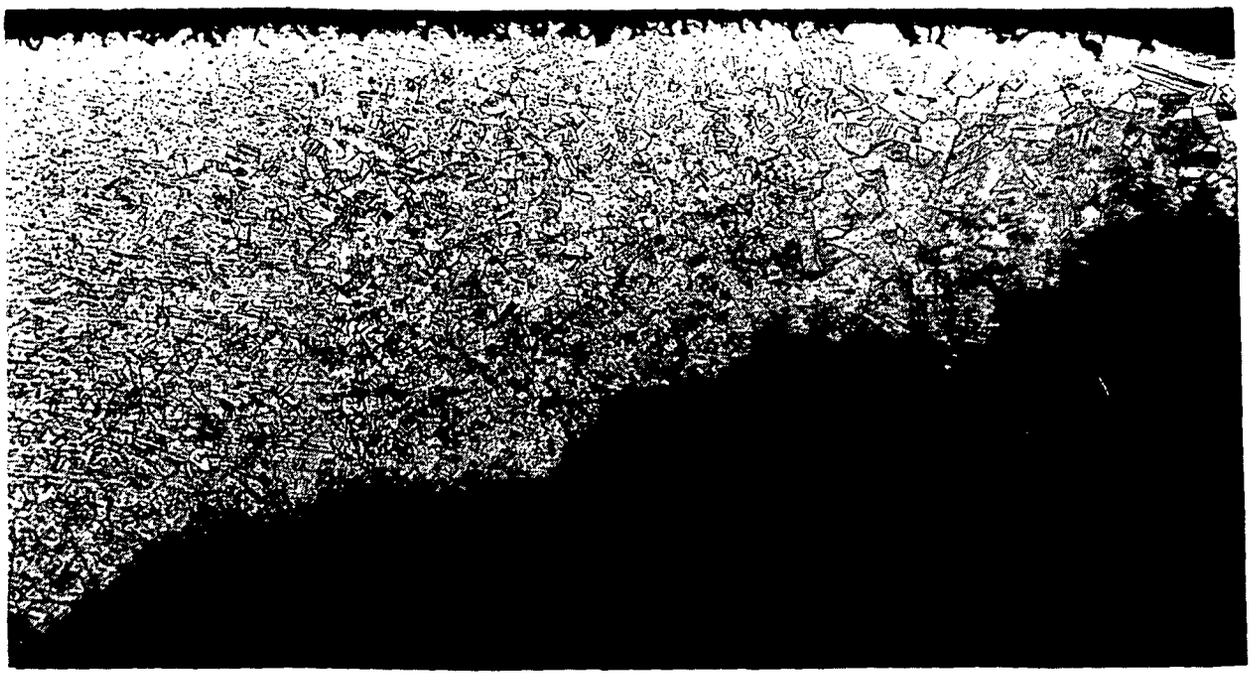

Figure 13. Metallographic Cross Section Showing Weld at Left, Heat Affected Zone (Center Right) and Parent Metal (Coarser Grain Structure — Right) in Tube at Location 1 (Figure 8). The Top of the Photomicrograph Shows the Shallow Grain Boundary Pitting Attack at the Outside Tube Surface and the Bottom of This Section Shows the Deeper Attack on the Inside Tube Surface

CONCLUSIONS

The catastrophic failure of the wash liquor tubes was caused by severe chloride attack in the form of pitting, stress corrosion cracking and crevice corrosion. That this attack is more concentrated at the U-bend and inside the tube is considered to be the result of fibrous deposits which accelerate attack by crevice action. In addition, this location coincides with the area of highest residual stress and operating stress as well as stresses arising from corrosion product wedging. In the presence of chlorides, pits form very rapidly in preferred

or under deposits and act as effective notches or points of stress concentration. Stress corrosion cracks develop at these sites and propagate rapidly to failure (Fig. 12).

The bottom portion (shell side) and U-bend section (tube side) are favorable locations for crevice corrosion because of the following reasons. The liquor flow is slow. Solids concentrate by settling. Drainage or outflow is poor during downtime leaving stagnant conditions. In addition, the fibrous deposit serves as an effective "wick" to draw and concentrate any harmful species from the environment — in this case the chloride ion.

RECOMMENDATIONS

1. Analysis of heater liquors for chloride content should be performed regularly.

2. The use of inhibited muriatic or hydrochloric acid as a cleaning agent has a long recorded history of serious corrosion problems. Regardless of the type of inhibitor, its use is always dangerous from a corrosion standpoint. Despite careful cleaning procedures, the design of equipment, with regard to stress, drainage and crevices renders the equipment vulnerable to chloride attack. Once small pools of the chloride solution are permanently isolated in pockets or under fibrous deposits due to poor drainage or ineffective scale removal, it is simply a matter of time for the occurrence of this attack. The rate of corrosion and its severity will then depend upon inhibitor decay, presence of passivating agents, and local flow rates.

Although other cleaning agents, e.g., inhibited citric, sulfuric, sulfamic or nitric acid, and other agents are more costly and more difficult to handle, their

use may be justified relative to the cost and total service life of the stainless steel equipment.

3. If continued use of inhibited hydrochloric acid is necessary, the following procedure is recommended (13-15):

a. Analysis of scale deposit to ascertain its reaction products with hydrochloric acid. For example, the reaction products may themselves be corrosive or decompose the usual inhibitors.

b. Inhibited HCl acid should never be used above 60°C (140°F).

c. Close supervision and monitoring of the acid cleaning process is essential (16).

d. After cleaning, high pressure flushing water should be used for a period of time at least equal to that of the cleaning period.

e. After water flushing, the last traces of acid, if any, should be neutralized by reflushing with a solution containing suitable neutralizing and passivating agents; e.g., trisodium phosphate, borax, or caustic soda.

f. Final treatment consists of reflushing with water.

4. Type 304 stainless steel is not an acceptable material to contain environments high in chloride content. Suitable candidate materials for this application are Inconel 600*, E-Brite 26-1**, or 3RE60***, stainless steels. Cost of these materials for retubing both primary and wash liquor heaters is given in Table IX. Available data for Type 316L stainless steel tubing is also included. These materials have shown excellent performance in resisting chloride

*Trade name — International Nickel Company.
**Trade name — Airco Vacuum Metals.
***Trade name — Sandvik.

attack, caustic embrittlement, and crevice corrosion. E-Brite 26-1 alloy is recommended for this application.

TABLE IX

TUBE MATERIAL COST AND DELIVERY

Primary Heater

Type	Manufacturer	Description	Cost
E-Brite 26-1	Airco Vacuum Metals	310 PCS 16 BWG 1-1/4 inch diameter	$16,640
Inconel 600	Huntington Alloys	310 PCS 18 BWG 1-1/4 inch diameter	$24,489
3RE60	Sandvik Steel	310 PCS 16 BWG 1-1/4 inch diameter	$19,856
316L	Carpenter Steel Co.	310 PCS 18 BWG 1-1/4 inch diameter	$10,781

Wash Liquor Heater

E-Brite 26-1	Airco Vacuum Metals	160 U-bend 18 BWG 1 inch diameter	$12,742
Inconel 600	Huntington Alloys	160 U-bend 17 BWG 1 inch diameter	$24,192
3RE60	Sandvik Steel	160 U-bend 18 BWG 1 inch diameter	$23,450[a]
316L	Carpenter Steel Co.	160 U-bend 18 BWG 1 inch diameter	$10,500

[a]This cost includes bending the tube.

RECOVERY FURNACE BOILER TUBES

In the kraft recovery process, gases from the combustion of black liquor furnish heat to generate steam in mild steel tubes. Corrosion of these tubes may occur either internally from improper feedwater treatment or externally (fireside) from corrosive elements in the gas. The steam generating section of the recovery boiler is a critical location for corrosive attack because it is subjected to particulate and scale accumulations and sometimes unfavorable temperature, composition, and combustion gas flow. Sootblowers and chemical additives are routine treatments to help reduce this attack and improve the efficiency of heat transfer in this section.

In the following case history, a change from kraft to 100% NSSC recovery caused a substantial increase in the corrosion rate of mild steel tubes in the generating section of the recovery boiler. Mild steel tubes provided years of excellent service during kraft recovery, but new tubes in the first and second passes had to be replaced after only sixteen months during the NSSC recovery process.

Although direct analysis or flow rate measurement of the combustion gas were not reported, higher sulfur contents would be expected in comparison with the kraft process (17). During inspection, scale was removed from the generating section tubes and found to be highly acid in nature. Attempts were made to reduce the acid condition by soda ash and magnesium oxide addition but this failed to decrease the corrosion rate. Upon retubing the first pass in the generating section, a small section of one of the failed tubes was obtained for failure analysis.

FAILURE ANALYSIS

The failed section of tube is shown in Fig. 14 (arrow points toward the thinned side of the tube). Corrosive attack on the exterior of the tube took the

form of localized thinning rather than uniform metal loss around the periphery. The corroded part of the outer tube surface was covered with a thin layer of brown deposit. The tube interior was uniformly covered with a thin, light gray deposit which was not further analyzed. Both surfaces (inside and outside) were smooth and free of any large surface disruptions or perforations. A small sample was cut from the corroded area for closer examination using the scanning electron microscope (SEM) and for identification by x-ray diffraction.

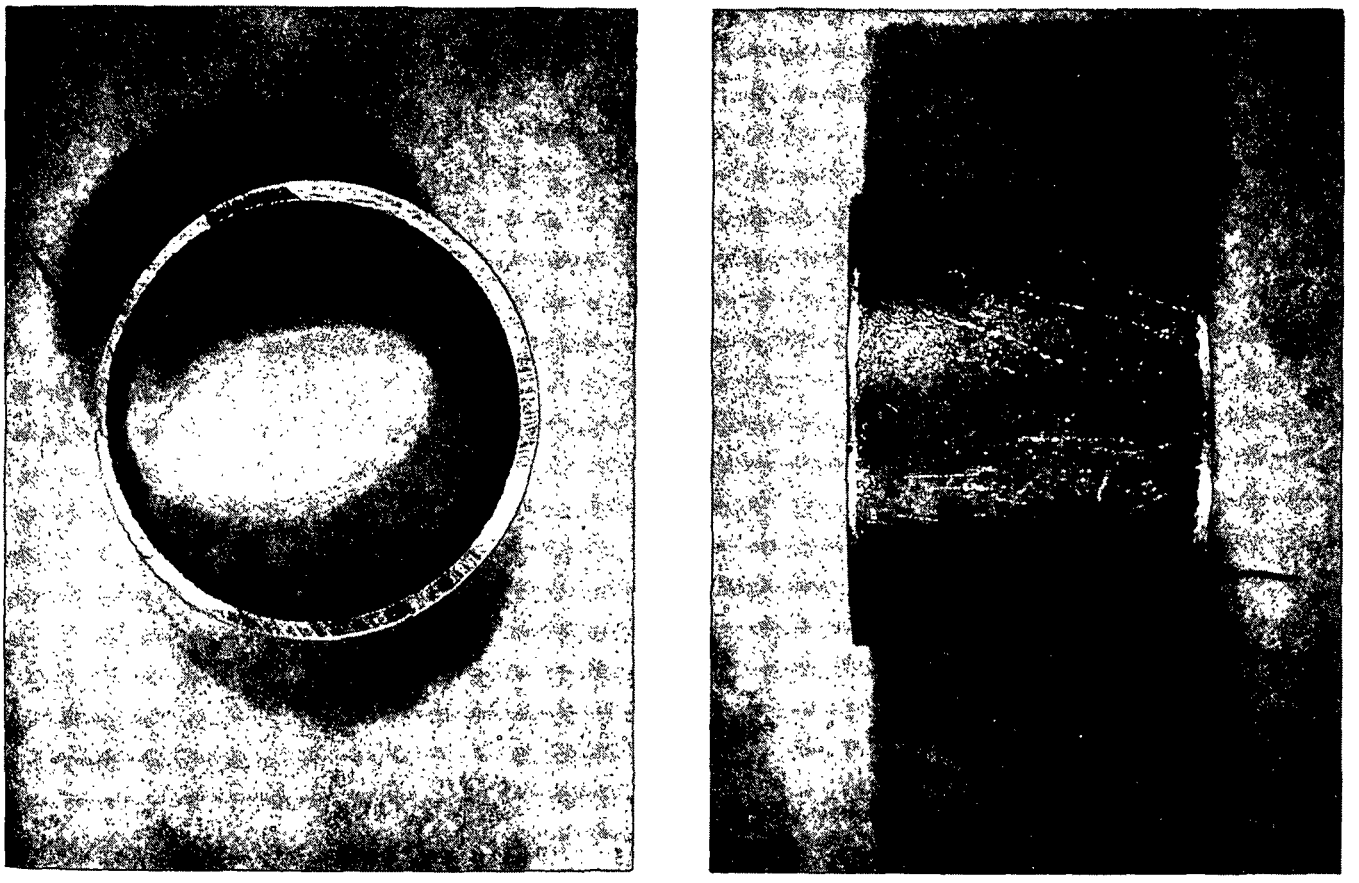

Figure 14. Photographs of the Cross Section and Exterior of the Tube Which Failed Due to Fireside Corrosion. The Arrow Points Toward the Thin Section of Tube and the Fireside Corrosion Products

The appearance of corrosion products under SEM magnification is shown in Fig. 15. Only a small fraction of crystalline particles is indicated. The x-ray spectra at this location (Fig. 16) shows a predominance of iron and sulfur and small amounts of silicon, calcium and potassium.

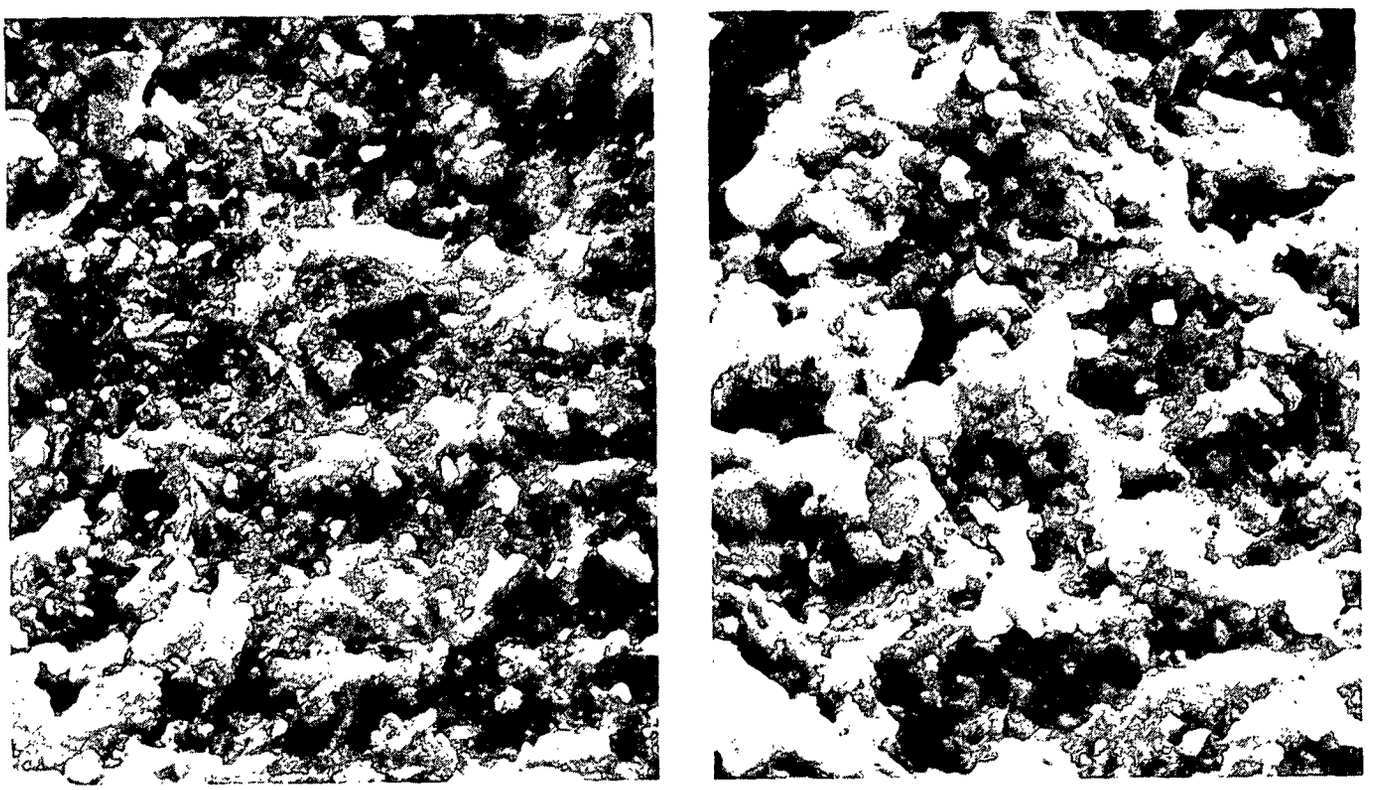

Figure 15. SEM Photographs of the Corrosion Products at 2000 X. Note the Relatively Few Crystalline Particles Contained in These Products

An x-ray diffraction analysis was run on a sample of the deposit scraped from the side of the tube. The results indicated that the major portion of the sample was amorphous.

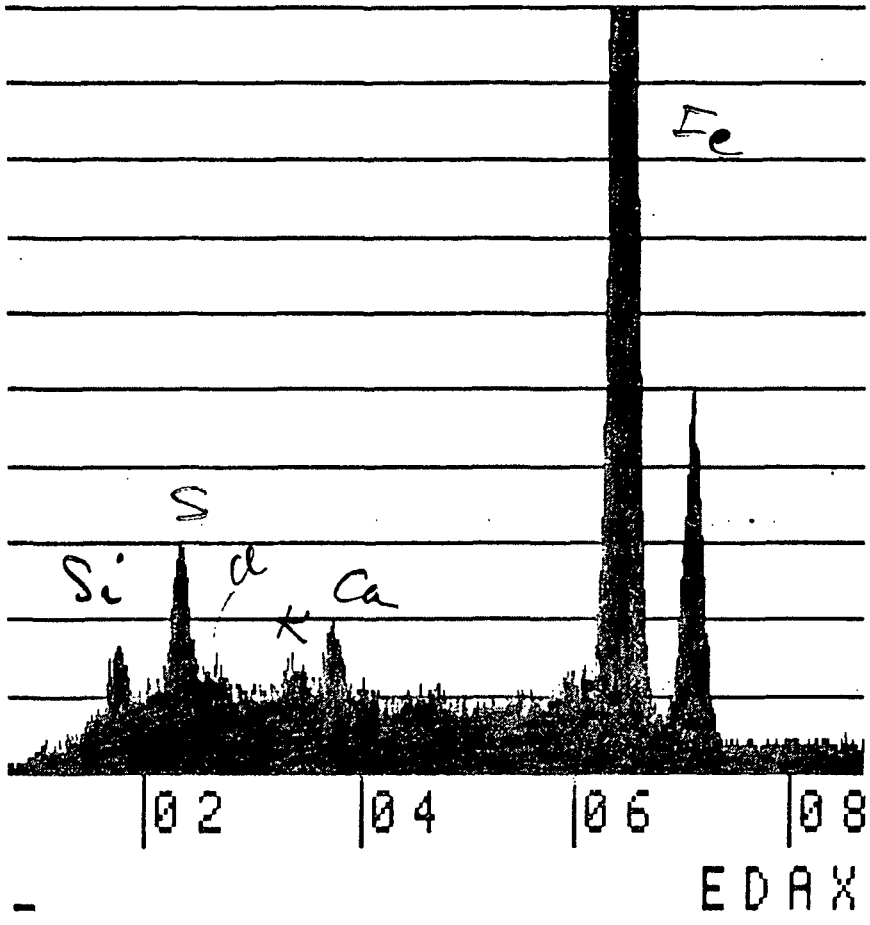

Figure 16. X-ray Spectra of the Corrosion Products at the Location of SEM Photomicrographs (Figure 2)

CONCLUSIONS

The excessive thinning of this mild steel tube is ascribed to corrosion by sulfur compounds. Nonuniform or localized areas of attack are related to temperature effects and direction of gas flow. Based on the analytical results showing the presence of only small amounts of iron oxide, there is a strong possibility that the predominant film constituent is iron sulfide. In the presence of sulfurous gases, e.g., within the generating section, iron sulfide is readily formed. In this case, the iron sulfide films were thin, nonporous layers which were largely amorphous. This type of deposit was confirmed by SEM, x-ray

spectra, and x-ray diffraction results. Iron sulfide films of this nature are unprotective. Increased temperature in local areas and higher gas flow rates would also accelerate the corrosion process.

The results of this investigation confirm those obtained by the mill. The major cause of corrosion was the sulfurous gases rather than the acidity of sticky fireside deposits. It also explains why the pattern of tube thinning was strongly influenced by the flow of these gases.

RECOMMENDATIONS

Sulfide corrosion can be controlled by either alloying the metal or lowering the sulfur content of the gases. The latter method is certainly the most economic and in this case it was selected to eliminate the problem.

To lower the concentration of sulfurous gases, a change in liquor composition was made by the mill toward reduced sulfidity. Their latest report indicates no metal loss on generating tubes within the time frame for the process change to take effect.

ELECTROSTATIC PRECIPITATORS

Electrostatic precipitators play a vital role in air pollution abatement by removing solid particulates from the recovery furnace flue gas. Precipitator construction consists of an electrical charging unit at gas inlet points, a series of upper and lower discharge wires and collector plates, rapper hammer assemblies to dislodge the collected saltcake, a collection hopper, and a discharge unit. Corrosive attack is particularly troublesome in the lower sections of the precipitator when inadequate insulation and sealing allow gas condensation.

In the failure analyses which follow, mild steel was used in the collection hoppers and low alloy, high strength steel was used in the rapper assemblies. The precipitator handles flue gas from a kraft recovery boiler. Severe corrosive attack on the lower walls and floor of the collection hopper as well as rapper hammer bolt failures at the lower level prompted the following investigation.

FAILURE ANALYSIS

Samples of thick, multilayered corrosion products were taken from the lower walls and access doors for identification by SEM and x-ray techniques. Figure 17 shows a cross section of one of these samples; six layers are evident in this sample. Layer 1 is composed of saltcake; its structure and composition by x-ray spectra is shown in Fig. 18. The high sodium and sulfur peaks are associated with the high content of Na_2SO_4. Figure 19 (top left) is an overview of the first three layers, and the successive pictures are progressive enlargements of Layer 2. Previous studies of metal oxide structures have shown that the morphology in Layer 2 is typical of αFe_2O_3 (18). This reaction product represents corrosion under highly oxidizing conditions. Layer 3 (Fig. 20) contains some salt

but it is predominantly composed of αFe_2O_3. Progressing inward toward the steel surface of the collector hopper, Fig. 21 shows the crystalline appearance of Layer 4 which is identified as Fe_3O_4 (18). The x-ray spectra of Layers 5 and 6 (Fig. 22) indicate no substantial change from Layer 4.

Figure 17. Cross Section of Corrosion Product Removed from South Wall of Precipitator A. The Six Layers were Analyzed for Composition and Structure

Saltcake samples taken from the same regions as that of the corrosion products were also analyzed. These samples were high in moisture content and in addition to high sulfate, the samples contained 1 to 2% carbonate.

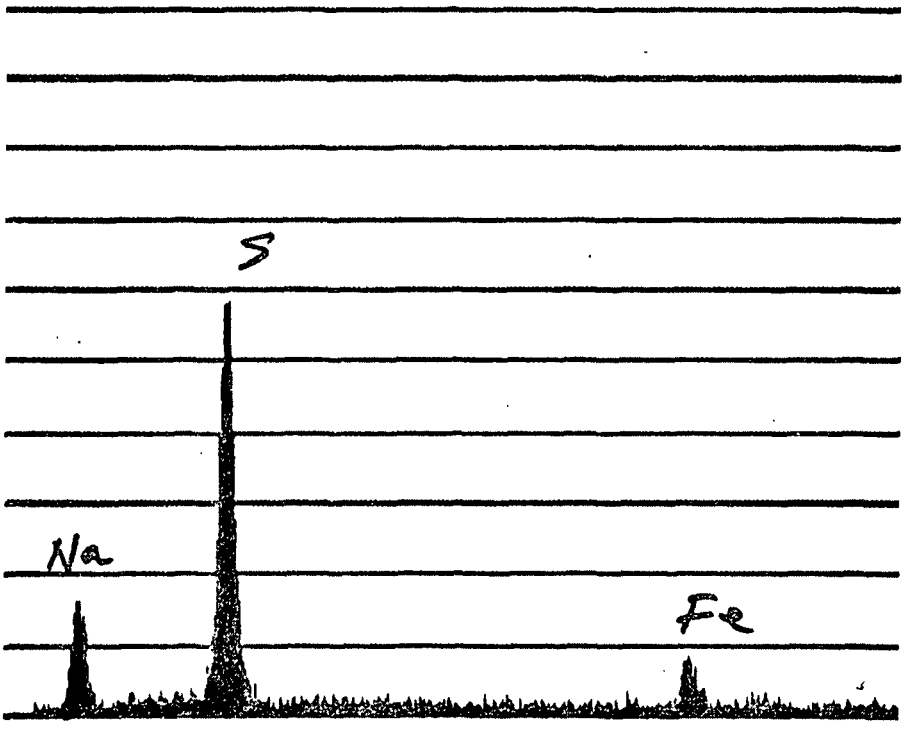

Figure 18. Structure and X-ray Spectra of Layer No. 1 (Saltcake Side)

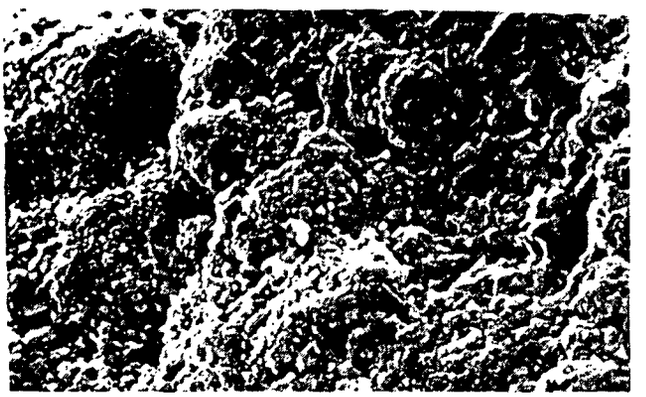

General Overview (500X)

Layer 2 Isolated (300X)

700X

3000X

10,000X

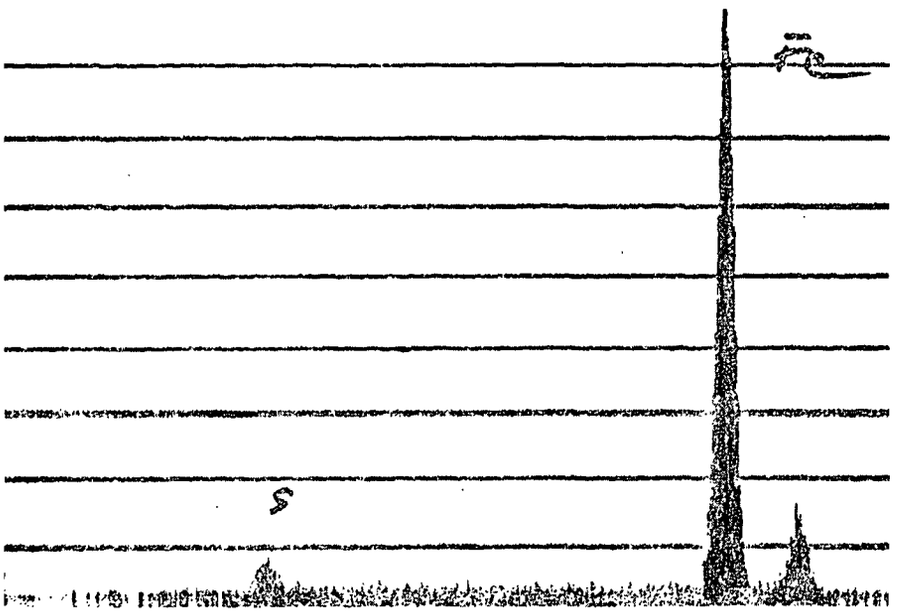

Figure 19. Composition and Structure of Layer No. 2 — First Layer Beneath Saltcake. Analysis Indicates This Product to be αFe_2O_3

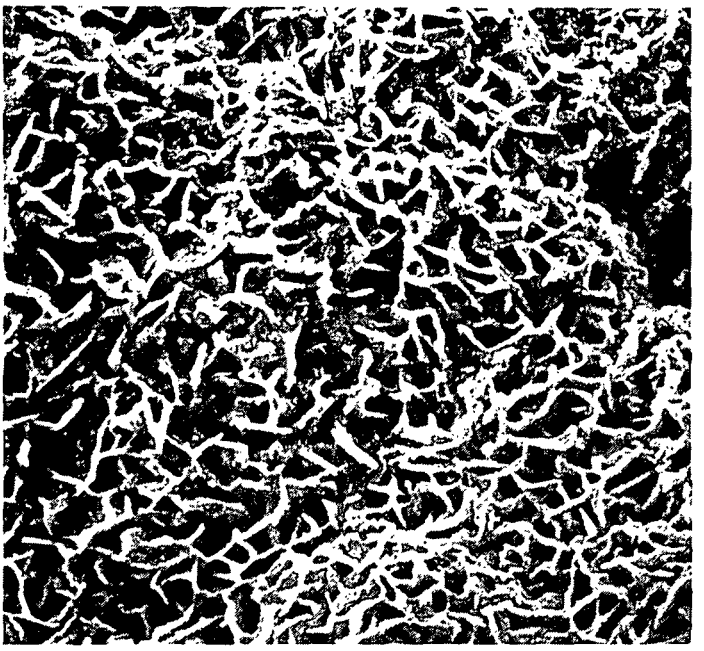

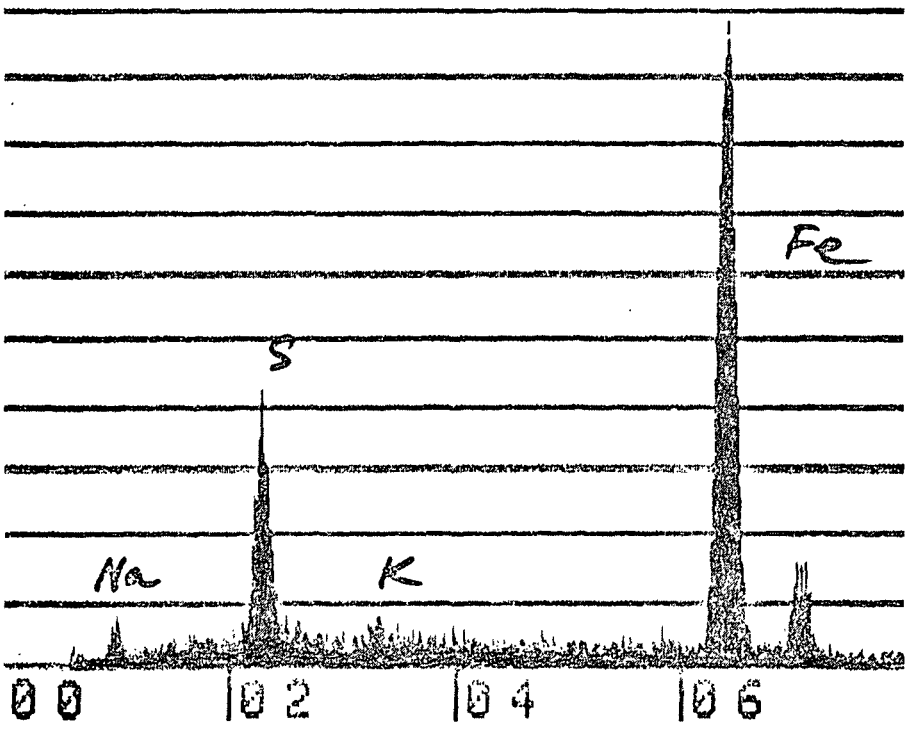

Figure 20. Composition and Structure of Layer No. 3

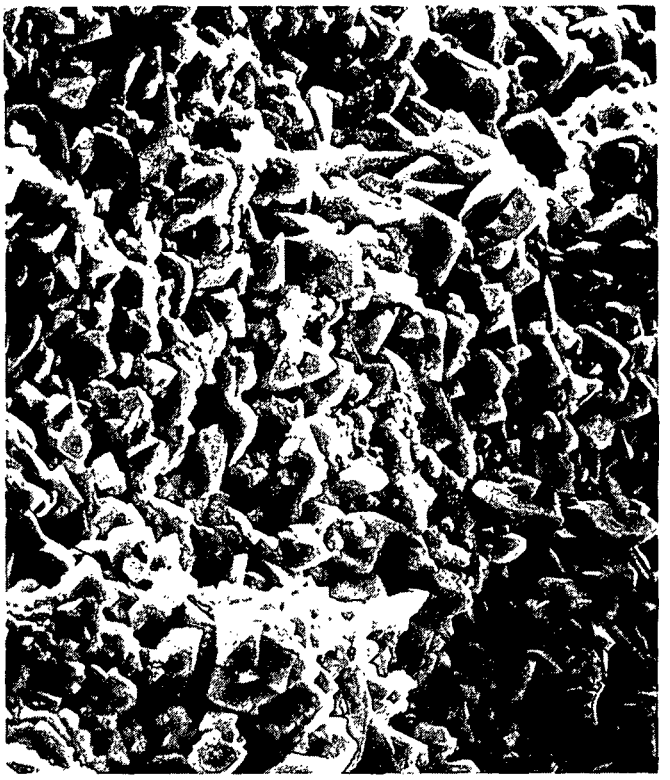

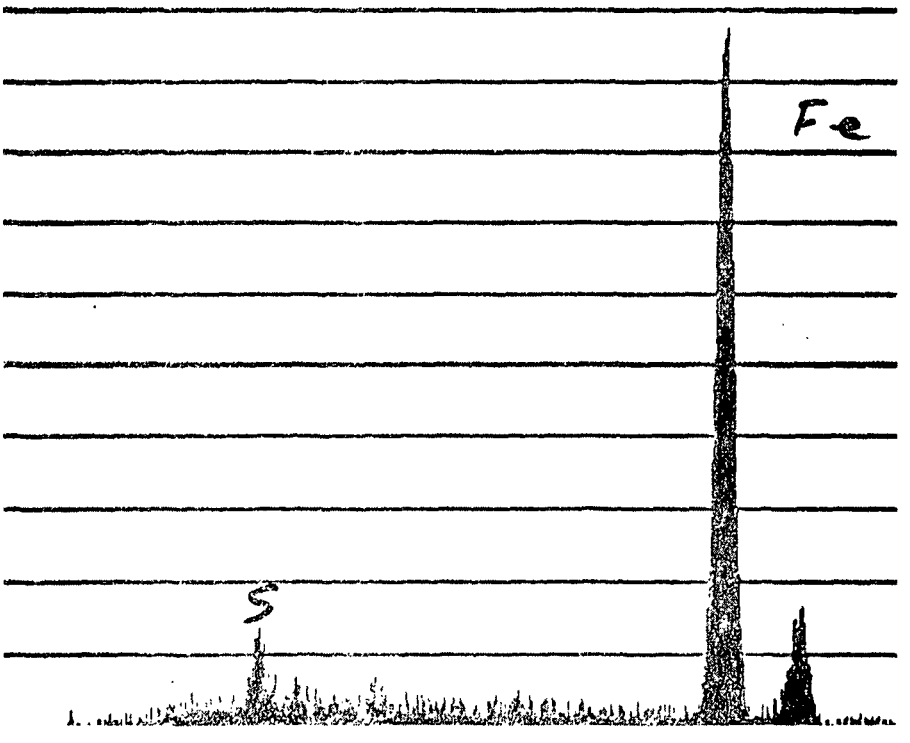

Figure 21. Composition and Structure of Layer No. 4 — Identified as Fe_3O_4

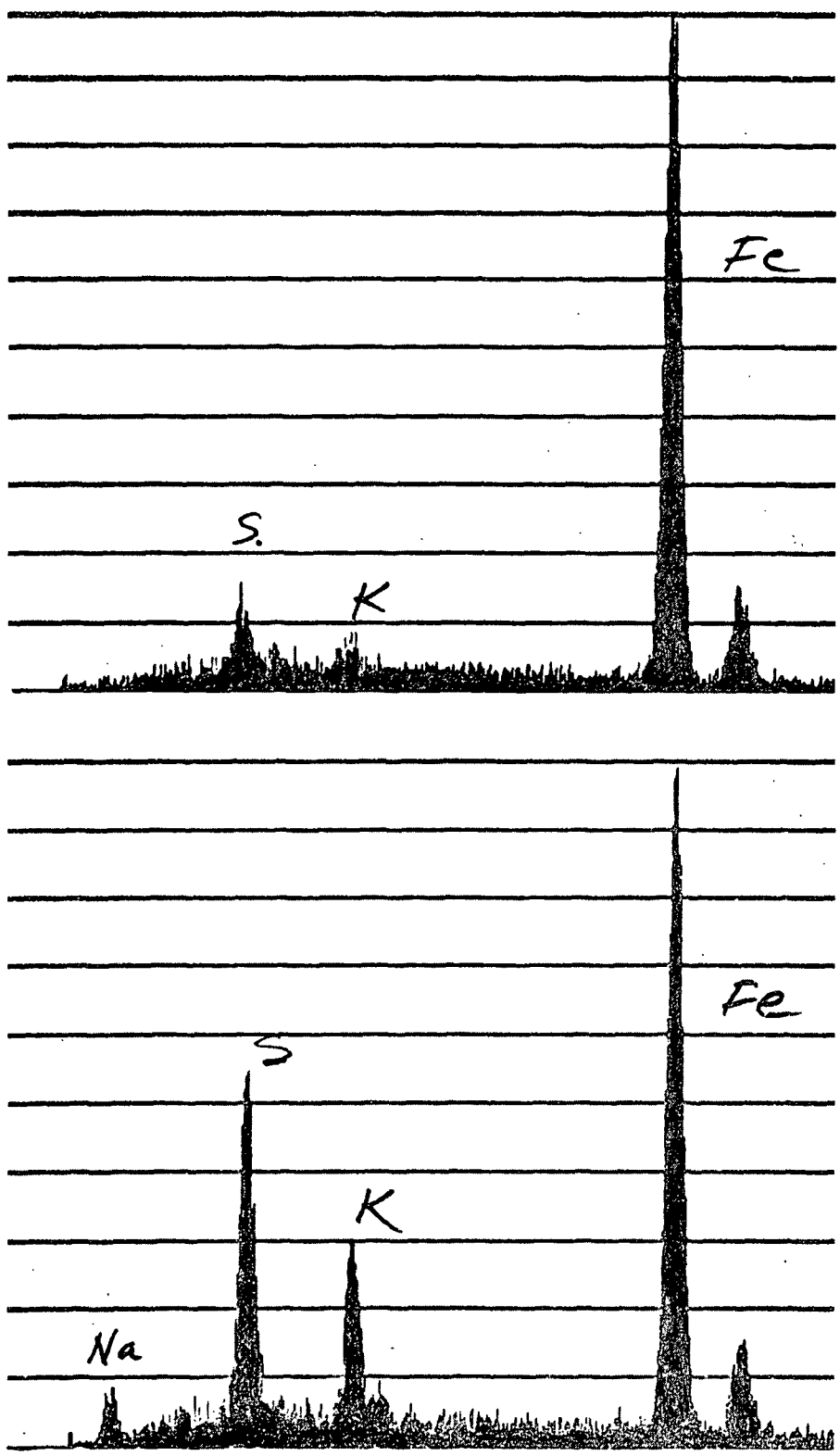

Figure 22. X-ray Spectra of Layers 5 and 6. The Structure was Similar to Layer No. 4 (Fe_3O_4), Thus, No Photographs were Required

It was not possible to obtain thickness measurements on the lower walls of the precipitator but based on the thickness of corrosion products, approximately 1/2 of the cross section had corroded away. This corresponds to a corrosion rate greater than 140 mils per year which is unusually high for this application.

CONCLUSIONS

The cause of this corrosion problem was related to entrained air from poor seals around the doors, low gas temperatures and inadequate insulation. This results in gas condensation and moisture which in combination with the sulfate-carbonate saltcake produces an acid condition. A slightly acid or neutral pH condition in the presence of oxygen greatly accelerates the corrosion rate of mild steel.

RECOMMENDATIONS

1. Continued efforts to improve the operating conditions within the precipitator by sealing and insulation are encouraged. The elimination of moisture and the prevention of below dew point gas temperatures will reduce the corrosivity of the environment.

2. The installation of thermocouples to monitor temperatures in the various sections is recommended.

SUBSEQUENT FAILURE ANALYSIS

In the previous study, extensive corrosion in the lower sections of the electrostatic precipitators was associated with condensation causing excessive oxidation of the mild steel hopper wall construction. It could well be that this corrosive attack was, in part, responsible for the failure of rapper hammer

assemblies which were reported a few months later. Inspection disclosed the location of failure was in the lower level rapper hammer units and it was caused by fracture of the attachment bolts. Broken sections of several bolt and nut assemblies were found downstream from the precipitators and one of these was obtained for failure analysis.

The failed bolts fractured through the thread just inside the nut. The overall surface of bolt-nut sections shows products of corrosion and light colored deposits in the threaded area. The fracture surface appears smooth and there are two different regions of fracture morphology (Fig. 23). The major region (extending over 50% of the fracture area) contains a series of parallel lines similar to fatigue situations. This region terminates in the second region which is devoid of markings and lower in elevation than the major one.

One of the bolt sections was analyzed for chemical composition and hardness. Sections of the fracture surface were examined optically and the non-fracture area, metallographically. The bolt material must meet ASTM specification A354, Grade BD which calls for alloy steel material, quenched and tempered to 32-38R_c hardness. There is no alloy chemistry specified except P and S at <0.04%.

The chemistry and hardness of the bolt material is shown in Table X. The composition is typical to that for AISI 4135 and the hardness complies with that specified.

The photomicrograph in Fig. 24 shows a tempered martensite structure which is characteristic of a liquid quenched and tempered heat-treatment — also as specified. A sulfide stringer type inclusion (resembling a "night crawler" worm) is also noted in the upper portion of the photo. However, the strength of the metal should not be impaired provided the inclusion count is low.

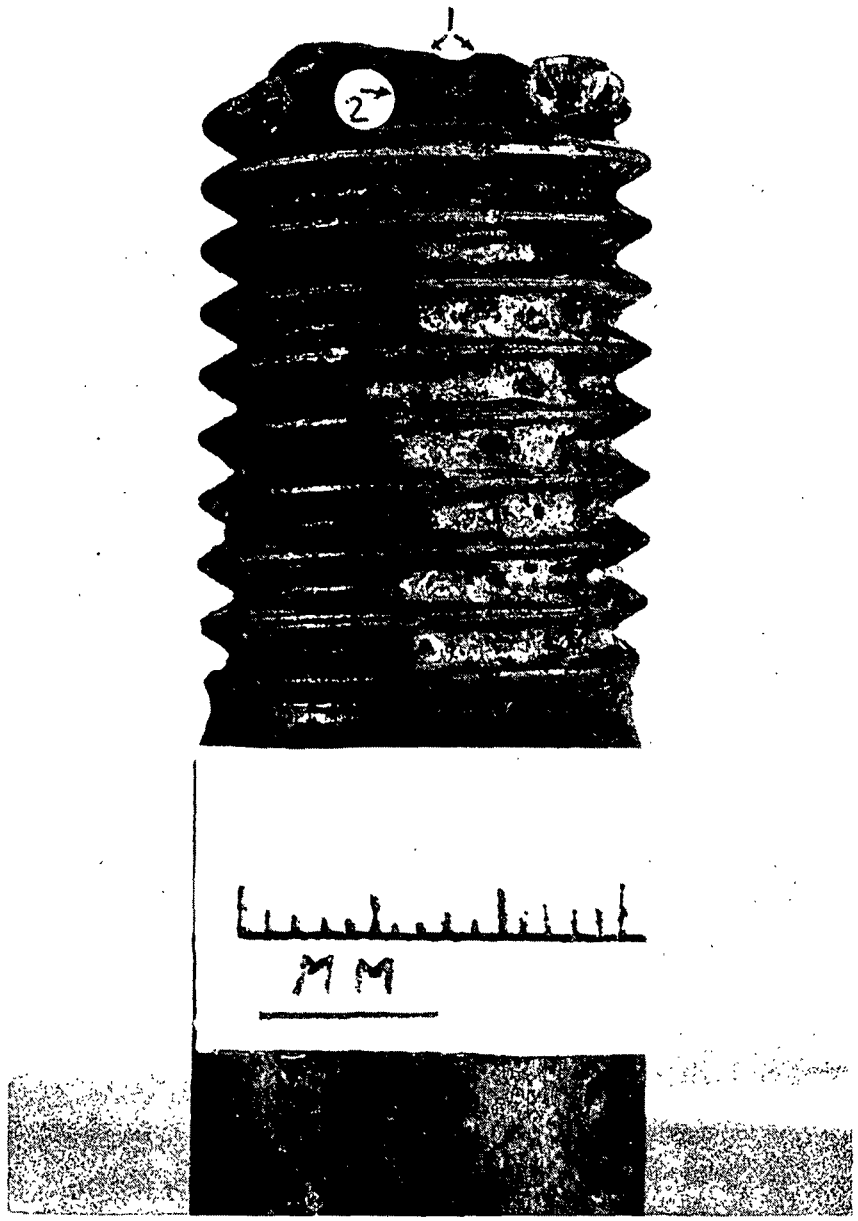

Figure 23. Photograph of the Fastening Bolt Which Failed in the Rapper Hammer Assembly in the Electrostatic Precipitator. Note the Heavily Encrusted Threads and Two Regions of Fracture Morphology. Region 1 Extends Over the Major Portion of the Fracture and it is Covered With Fatigue Striations. Region 2 is the Final Ductile Fracture Area

TABLE X

CHEMICAL COMPOSITION AND HARDNESS OF
BOLT MATERIAL

Item	Chemistry C	Mn	Si	P	S	Cr	Mo
Bolt	0.35	0.73	0.21	0.007	0.028	0.80	0.16
ASTMA 354 Gr. BD	--	--	--	0.04	0.04	--	--
AISI 4135 Typical	0.33-0.38	0.70-0.90	--	--	--	0.80-1.10	0.18-0.25

	Hardness (R_c)
ASTM 354 Gr. BD	32-38
Bolt	33.0, 35.0, 34.0, 34.5

Mechanical Properties Specified
Grade BD

Tensile Strength, psi	Yield Strength, psi	Elongation, %	Reduction of Area, %
150,000	125,000	14	35

Figure 25 is a macrophotograph of the fracture surface. It shows that the major portion of the fracture was caused by fatigue. This region of fatigue fracture terminates in the two final fracture areas which appear as shear lips at the top and bottom portion of the bolt.

This same sample was sectioned and viewed under scanning electron microscope (SEM) magnification. Figure 26 is a photograph of a possible site of crack initiation and the striated area of crack propagation. The crack appears to have initiated at the root of the thread then propagated by the fatigue action created during the rapping sequence. Figure 27 is a close-up view of the thread root area where pitting corrosion is evident. Within the region of fatigue crack

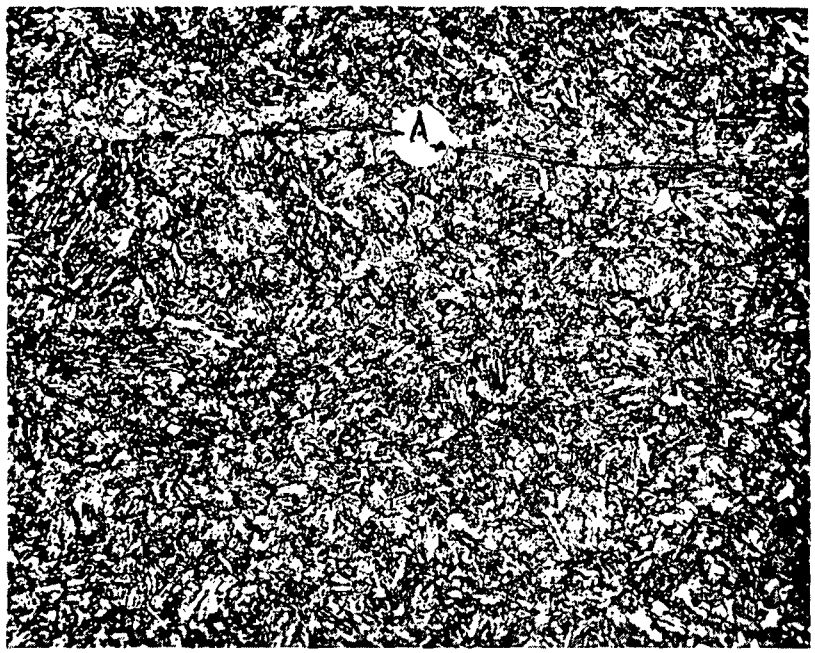

Figure 24. Photomicrograph Showing the Metallurgical Structure of the Bolt is That of Tempered Mortensite. Note Stringer Type Inclusions in Region Labeled A

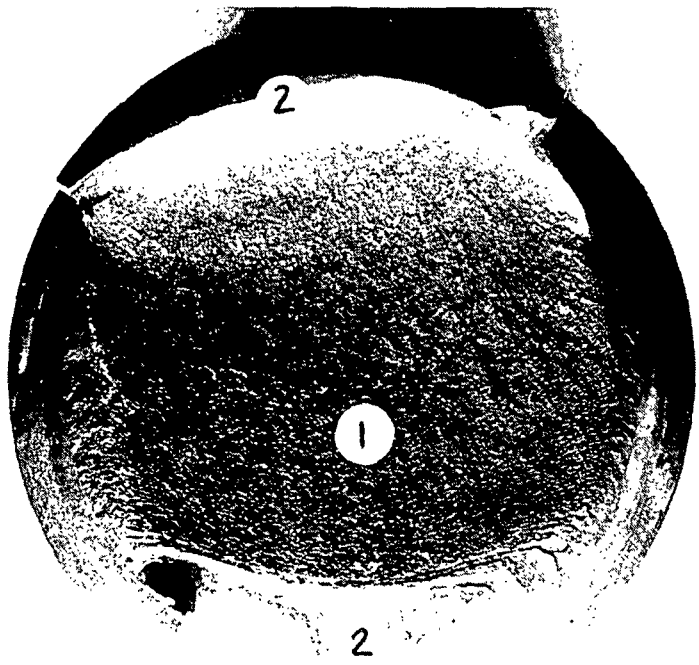

Figure 25. Macrophotograph Showing the Two Regions of Fraction Surface Morphology — The Fatigue Region Labeled 1 and the Last to Fail Ductile-Tensile Region Labeled 2

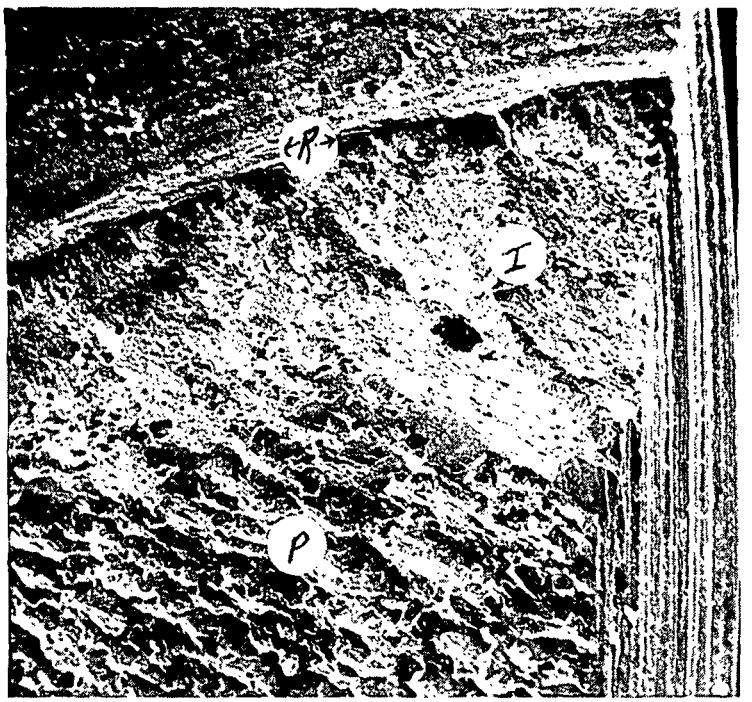

Figure 26. SEM Photomicrograph Showing a Region of Fatigue Crack Initiation (Labeled I) at the Thread Root (Labeled R) and the Crack Propagation Area (Labeled P)

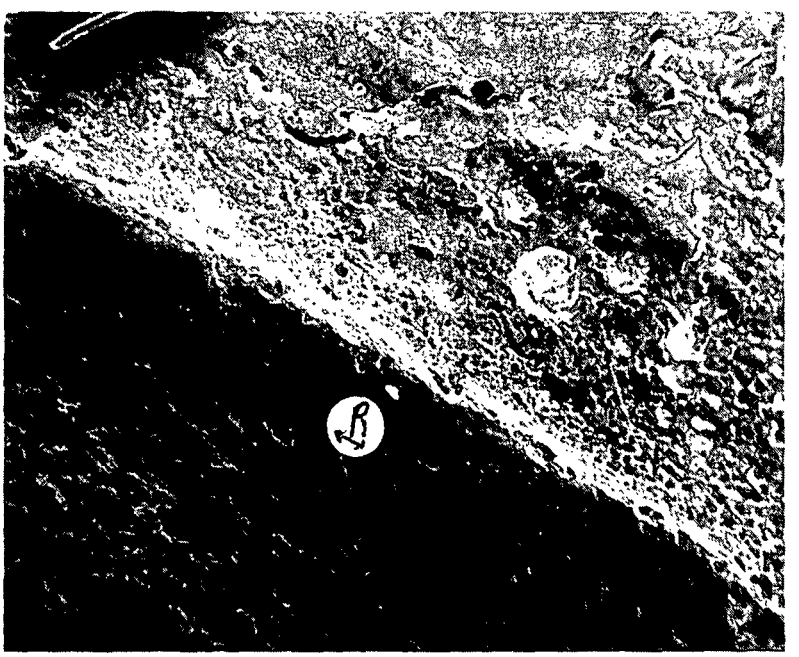

Figure 27. Close-up View by SEM Microphotography Showing Pitting and Crevice Corrosion Attack Within the Thread Root Area (Labeled R)

propagation, Fig. 28 shows numerous secondary cracks and corrosion pits along the major crack front.

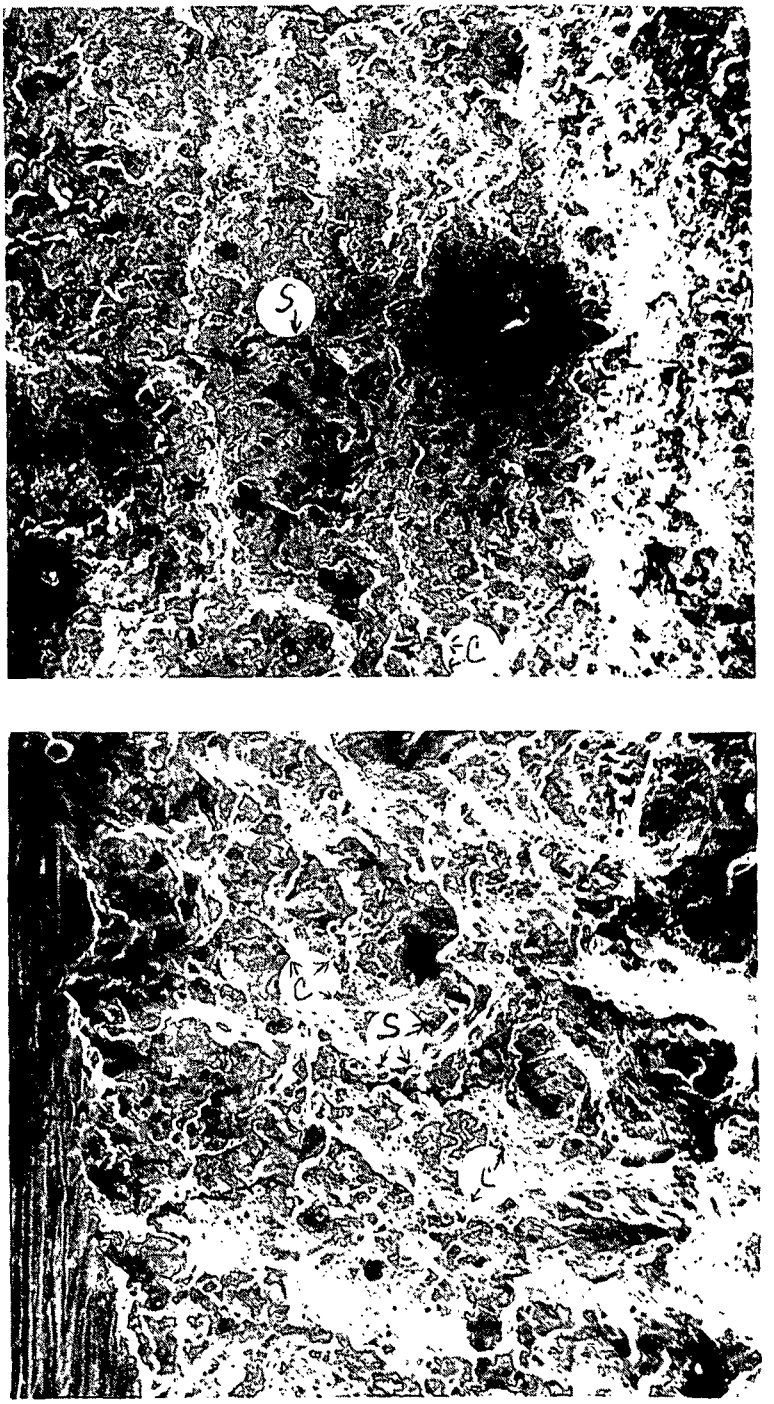

Figure 28. SEM Photomicrograph of the Region of Fatigue Crack Propagation. Upper Photograph at 100X and Lower Photograph at 200X. Secondary Cracks (Labeled S) and Corrosion Pits (Labeled C) are Seen Throughout These Striated Regions

CONCLUSIONS

The bolt failed by a corrosion fatigue process. The root of the thread serves as an effective site for crevice corrosion. This fracture location is also a region of high stress. Crevice corrosion and pitting assist crack formation by concentrating the stress at small, local regions. Once the crack is initiated, corrosion accelerates its growth along the major crack front and promotes secondary crack formation. These typical features of corrosion fatigue fracture were observed in the fractography presented.

The bolt-thread root immediately adjacent to the edge of the nut on the washer side is a common fatigue initiation site in threaded fasteners. Stress concentration is produced at this site because the bolt elongates as the nut is tightened, thereby producing increased loads on the threads nearest the bearing face of the nut, which add to normal service stresses (18). Thus, the total stress in this application is composed of the residual stress inherent in the bolt by the manufacturing process, the induced stress during fastening, the loading stress in service, and stresses caused by the wedging action of corrosion products along the major crack front.

There are at least two possibilities for the initiation of a corrosion fatigue crack. It may be the result of corrosive attack which forms an effective "notch" for the crack to originate, or it may start at some point of local surface damage caused by a forging defect, undercutting the thread, nonmetallic inclusions, etc. No definite cause can be ascribed to the initiation of this failure because the fracture surfaces were subjected to considerable damage before the broken bolt was found. The corrosion observed in the bolt-thread root area as well as that on the fracture surface could have occurred after the crack had initiated

and was well into the propagation stage. Based on these observations and past corrosion problems within the precipitator, one can only say that corrosive conditions were present to assist both initiation and growth of fatigue cracks.

RECOMMENDATIONS

1. Reducing the stress — The bolt-thread root stress concentration can be reduced by using nuts of a softer material that will yield and distribute the load more uniformly over the engaged threads (19).

2. Design — Significant improvements in fatigue life have been reported by rolling (cold working) the threads rather than cutting them (19). It is important that the rolling operation follow rather than precede heat treatment. This crevice corrosion problem can be eliminated by changing to an all-welded construction.

3. Materials — The corrosion resistance, corrosion fatigue, and impact strength are improved by alloying the steel with nickel. This could be achieved by a change to the 4300 or 4600 grades of alloy steel or by plating the present bolt material. Nickel plating or nickel-cadium plated fasteners of low alloy high strength steel (per AMS 2416) offer good corrosion resistance at temperatures between 450 and 900°F. The 5% Cr tool steels (H-11) have also been reported to retain high strength in fastener applications up to 900°F (19).

WEAR OF CORRUGATING ROLLS

In the past five to six years, there has been a dramatic increase in wear of corrugating rolls throughout the industry. This has resulted in a considerable loss in roll life. The advent of whole tree chipping and 100% recycle mediums as well as higher production rates are among the reasons given by roll manufacturers to account for reduced roll life.

The possibility of a combined action of corrosion and wear prompted an investigation of the upper roll of a corrugator which had to be removed after only eight months service. The roll was manufactured from SAE 4340 steel and heat-treated to 350-390 Brinell hardness. After final machining to a 32-63 RMS finish, hard chrome plate ($\geq$ 700 VHN) per AMS2406 was specified. The roll was approximately 12 inches in diameter by 88 inches long.

New rolls are subjected to simulated "normal wear" or "break-in" prior to service. This is accomplished by "running-in" the bare rolls for approximately 30 minutes with a light covering of oil at normal operating pressures.

At a machine speed of 500 lineal feet per minute, the roll rotates at 160 rpm. It is not possible to define the exact magnitude of surface stress involved because of operating variables, alignment, loading and geometrical effects. However, these contributions as well as the high residual tensile stresses from flute machining during manufacture lead to high surface stress during operation.

The corrugating medium used on this roll was made from 100% recycled stock. The pH of the medium is 7.5 to 8. An analysis of the residue from the spreader bar after 107,000 consecutive lineal feet was reported by the mill to contain fiberglass and substances characteristic of materials used in wax and

water based coatings, e.g., polyethylene, polyvinyl acetate, ethylene vinyl acetate and paraffin. These contaminants cannot be entirely removed by the centrifugal cleaners used in stock preparation at the mill.

Lubrication consists of a light covering of oil by mist spraying Gulf Oil "Security 39," during operation. Heavier coatings of this oil are applied before prolonged shutdowns. Periodic cleaning (once each week) is accomplished by steam and heated soft water impingement followed by light oil applications. The medium is preheated with low quality (high moisture) steam (approximately 185°F) prior to corrugation. Rolls are heated internally with 170 lb steam, and temperatures of 340 to 360°F are achieved during the corrugating process.

FAILURE ANALYSIS

The overall size of the roll as received and partially uncrated is shown in Fig. 29. A section of the corrugating medium that was sent with the roll is shown taped across its surface to give perspective of working width. Overall visual inspection along the working width disclosed a complete loss of chrome plate in the flute valley, very thin coverage on the sides of the flute, and only isolated patches or specks of chrome plate remaining on the flute tips. Outside the working width at each end of the roll, the chrome plate was somewhat better preserved. A section (labeled A — Fig. 29) was cut from the roll for closer inspection.

Figure 30 shows Section A removed — the end of the roll is on the left side of the photograph. Visual examination of this section at low power magnification disclosed evenly distributed and highly deformed "waviness" along the flute tips. The "waviness" was in the form of brinnelling or peening across the tip. Also, pitting corrosion of the base metal was evident in these areas free of

chrome plate. The valley of the flute profile was worn free of chrome plate and discolored from base metal corrosion and deposits. The original machining lines were not evident in this area and isolated, randomly distributed pits were also detected. A thin but uniform covering of chrome plate was observed along the sides of the flute with randomly distributed pin holes or small punch marks penetrating this coating.

Figure 29. Photograph of Worn Upper Corrugating Roll as Received. The End Marked "A" was Cut From the Roll for Closer Inspection

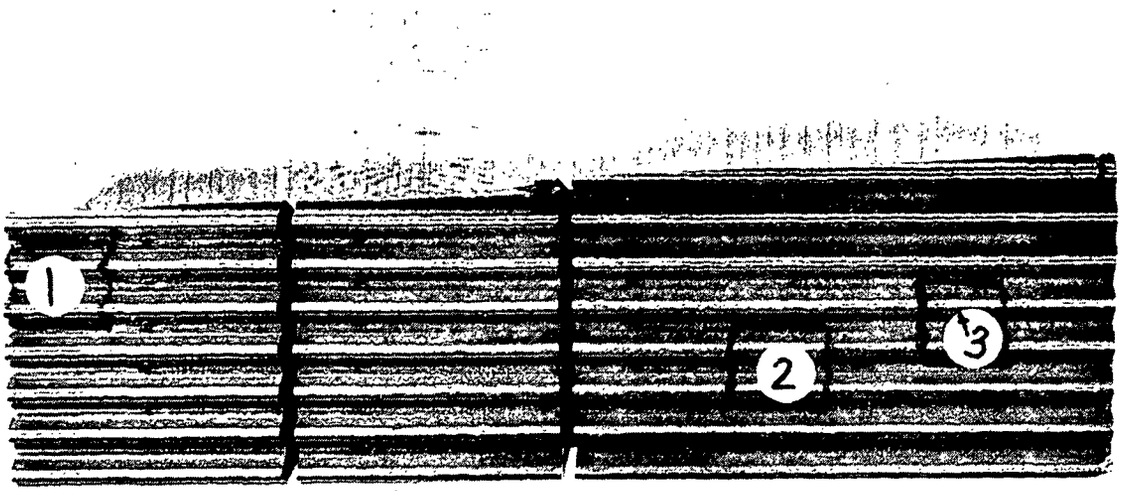

Figure 30. Photograph of the Section Cut from Location "A", Shown in Figure 13. Samples Marked 1, 2, and 3 were Removed for Further Analysis. Arrow on 3 Points to Speck of Chrome Plate

Smaller samples (labelled 1, 2, 3 in the photograph, Fig. 30) were cut from this section for microscopic and metallurgical analyses. Sample 1 is in the area outside the working width where there is better coverage of the chromium plating. Sample 2 is representative of the areas of greatest wear, lack of chrome plate and a pit located in the valley of the flute profile. The area of Sample 3 was selected because it contains a patch or speck of chrome plate on the flute tip (arrow points to it in Fig. 30) which was large enough to permit microscopic and metallographic analysis.

The samples were ultrasonically cleaned in acetone and examined by scanning electron microscopy (SEM). Figure 31 is a montage of Sample 1 extending from the valley (lower left side of photo) to the tip of the flute. Since this sample was from an area at the end of the roll, the character of the surface shown in the montage is essentially the result of metal to metal contact during service. The most severe surface degradation occurred in the valley where surface disruptions appear as holes and/or gouges. In this particular area there is a complete loss of chrome plate and the rolling and sliding action between flute tip and valley has worn the surface below the original machining marks. There appears to be less metal loss along the side of the flute (similar to the pitch line area on gears) as the machining lines still remain with a very thin but uniform chrome coverage. The area at the top of the flute shows isolated points of damage in the otherwise intact chrome plating.

Since the tip of the flute in Sample 1 appeared to retain the best characterization of the original chrome plate, a closer examination was made of this surface. Both good and bad areas were detected, and x-ray analyses were made of each. Figure 32 shows that even in areas where chrome plate appeared good small amounts of iron could be detected, indicating local regions of breakdown in the chrome plate. In areas of greater surface damage, a number of cracks in the chrome plate could be seen around points where the plate was completely dislodged from the surface (see Fig. 33). The x-ray spectra in this region shows the high degree of breakdown (high iron peak) as well as the presence of silicon and calcium.

The surface damage sustained inside the working width of the roll, Sample 2, was far greater than that at the end of the roll. There was a complete loss of chrome plate along the flute profile but as in Sample 1, the greatest

Figure 31. SEM Montage of Flute Profile in Sample 1 Showing the Surface Damage Sustained in Valley (Lower Left), Side (Center) and Tip (Top) of the Flute. Magnification 40X

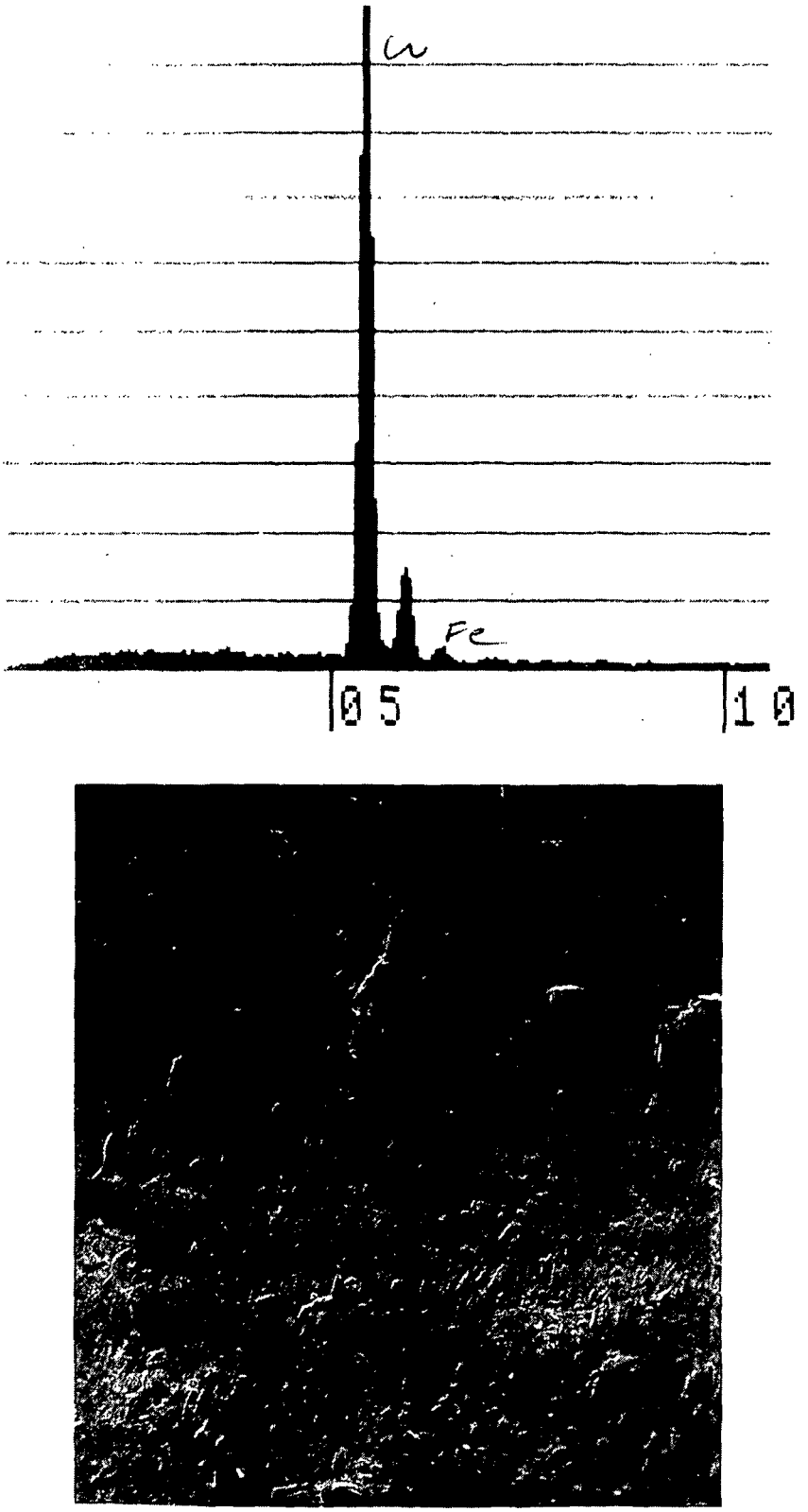

Figure 32. SEM Photograph and X-ray Spectra of a Local Region on the Flute Tip of Sample 1 Where Chrome Plate Coverage was Best. SEM at 200X

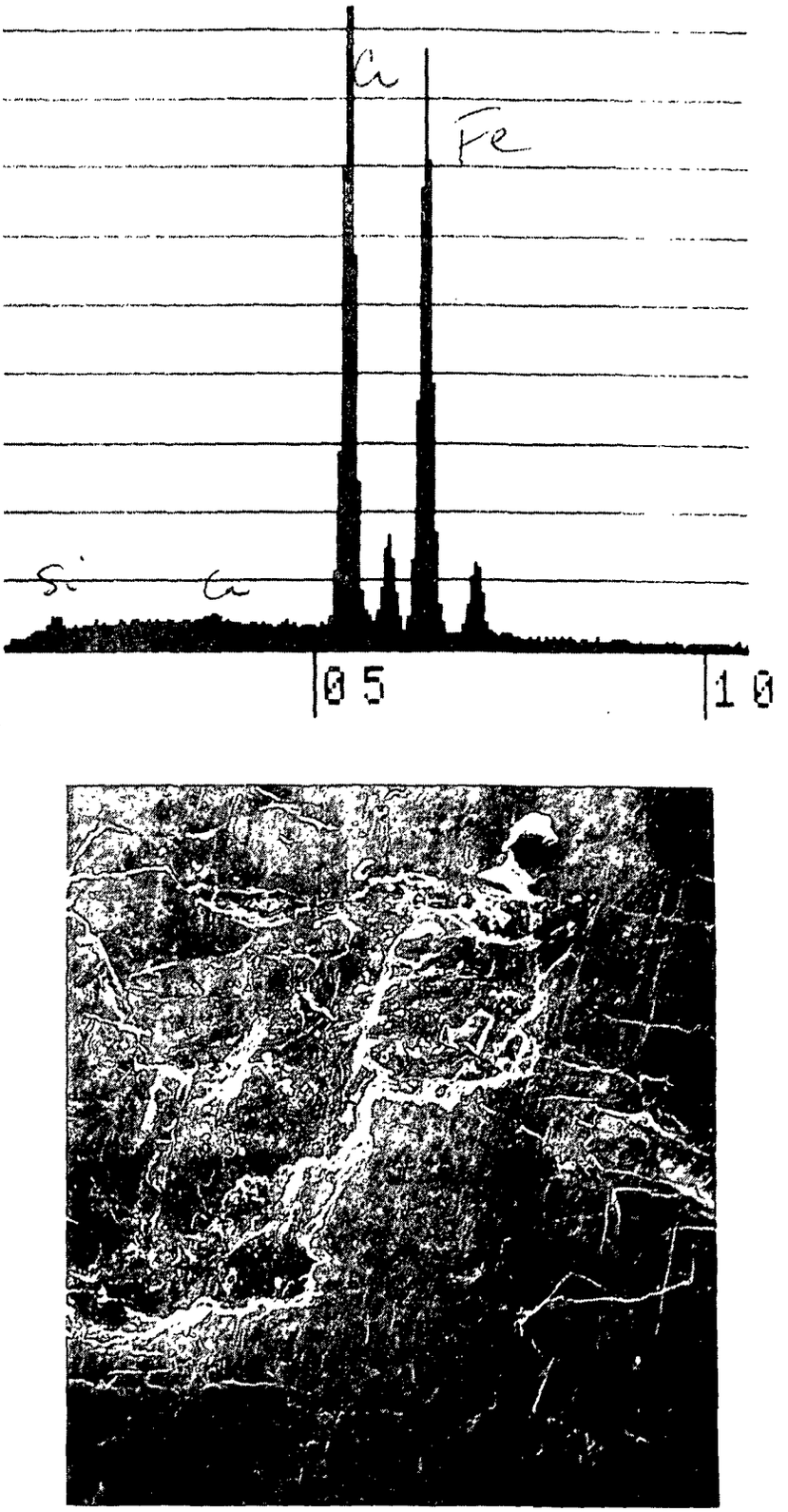

Figure 33. SEM Photograph (200X) and X-ray Spectra in a Local Region of Breakdown in the Chrome Plate. Note the Multitude of Cracks (White Lines Surrounding this Region

ERRATA

Page 63, line 5	Change Fig. 35 to Fig. 34
Page 63, line 8	Change Fig. 36 to Fig. 35
Caption, Fig. 34	Change Sample 1 to Sample 2
Page 66, line 2	Change Fig. 37 to Fig. 36
Page 66, line 5	Change Fig. 36 to Fig. 37

surface disruption was found in the valley and tip of the flute. The darkened pit noted visually in the flute valley of this sample turned out to be a circular discoloration under SEM examination (Fig. 34). Since this circular area is slightly depressed from the surroundings, it was probably not cleaned during sample preparation and thus appears dark. The photograph in Fig. 35 also shows that the extreme wear in the valley was in the form of "craters" (small areas of metal removal), and the sides and bottom of these craters were perforated with small holes. Figure 36 shows a close-up photograph of one of these craters. The x-ray spectrum of this region shows the base metal predominance (iron, chrome, nickel peaks) as well as the presence of silicon, calcium, phosphorus and sulfur. The calcium and silicon probably originate from the environment; e.g., corrugating medium, water, oil, while phosphorus and sulfur may be from the inclusions in the base metal.

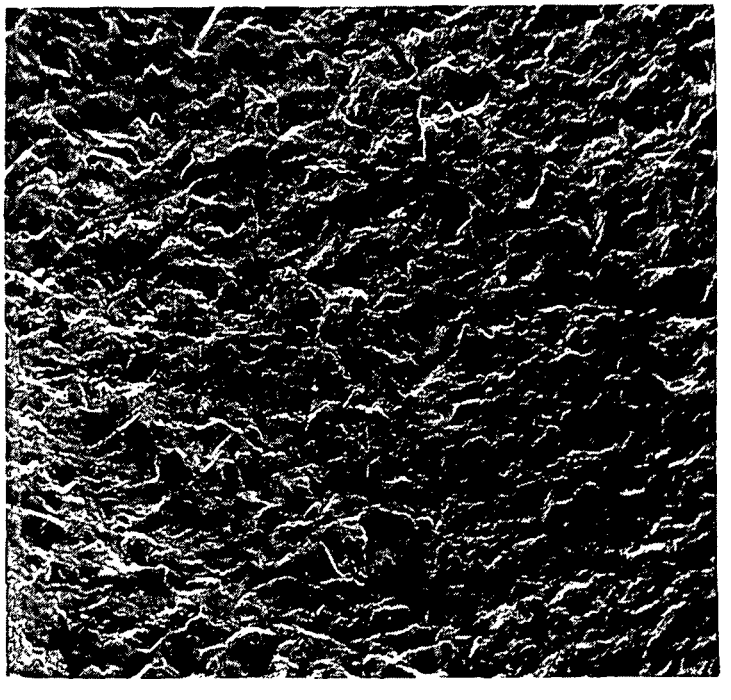

Figure 34. SEM Photograph (100X) of the Round Dark Area in the Flute Valley of Sample 1 Which Appeared to be a Pit Visually. This Photograph Shows it to be a Circular Discoloration Without Change in Surface Morphology from That of the Surrounding Area

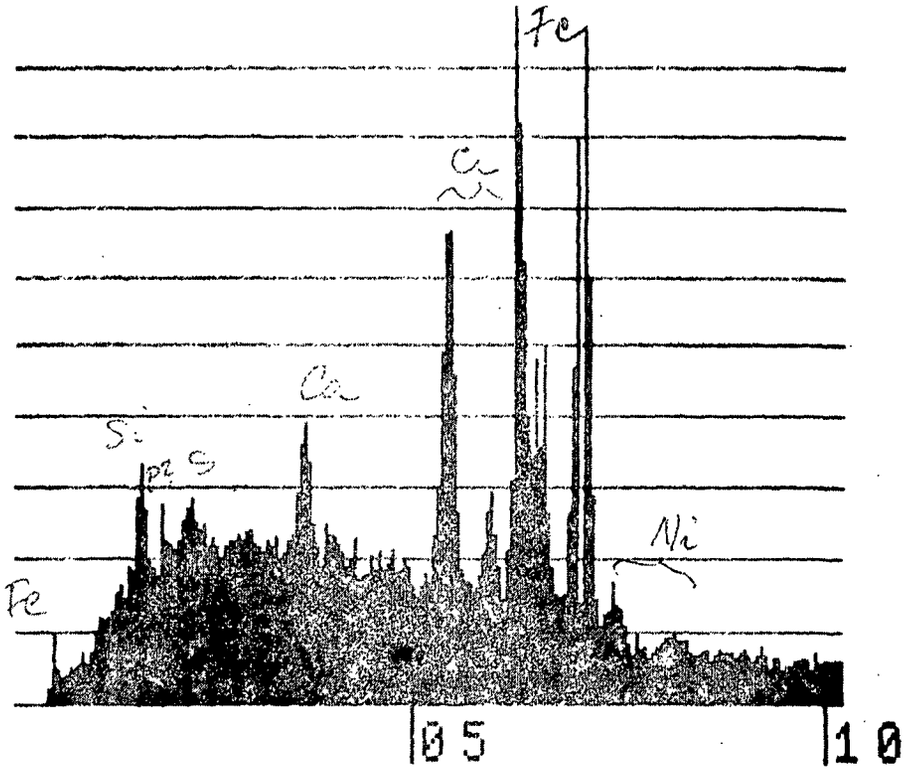

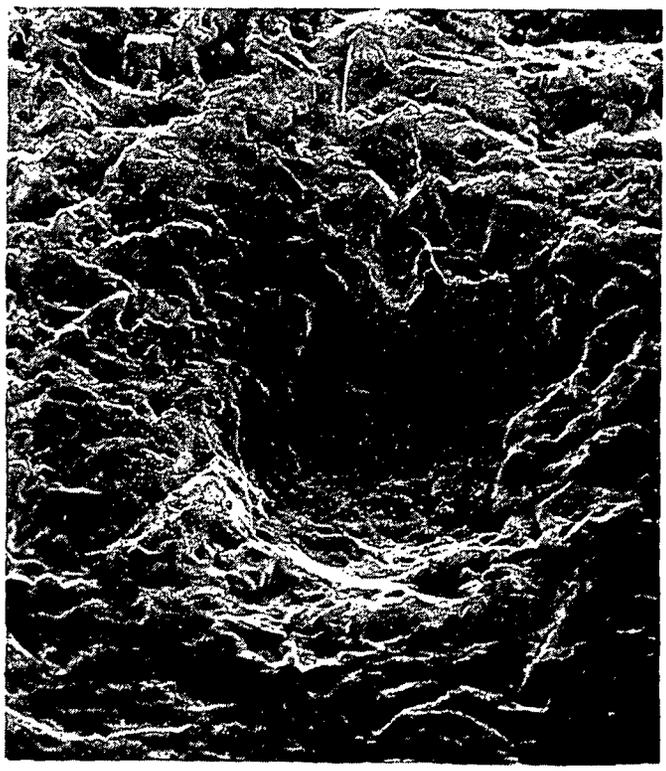

Figure 35. SEM Photograph (200X) and X-ray Spectra of the "Crater-like Surface Morphology Found in the Flute Valley of Sample 1

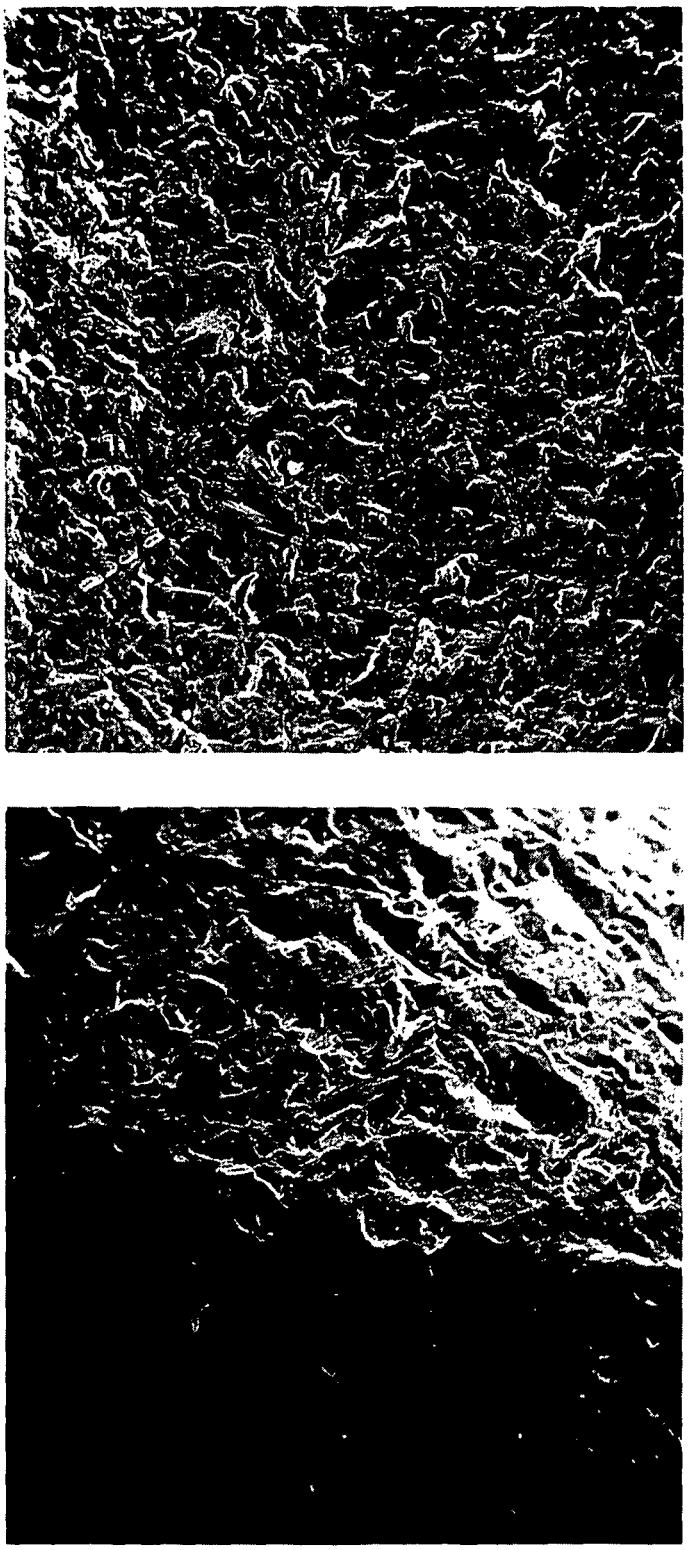

Figure 36. SEM Photographs (100X) of the Valley (Top) and Tip (Bottom) Surfaces of the Flute on Sample 3. The Perforated Craterlike Metal Removal on These Surfaces is Similar to That Found on Sample 2

The same type of severe deformation and surface disruption on flute tip and valley was found on Sample 3. Figure 37 shows the perforated crater pattern that exists in these areas. In addition, x-ray spectra of these regions in the flute tip area confirms the presence of the same elements found in the valley, namely, high iron peak (base metal exposure), silicon and calcium (Fig. 36).

Although the surface damage along the side of the flute was less severe than valley or tip, the craterlike appearance of the surface prevailed. Figures 38 and 39 are photographs of typical regions in these areas. In addition to the elements found previously, aluminum and potassium were also present in these areas.

There was an area of chrome plate on Sample 3 noted visually (see Fig. 30). This was confirmed by the x-ray spectra (Fig. 40) and the sample was sectioned in this area for metallurgical analysis.

The results of roll base metal analysis is shown in Table XI. The chemical composition and hardness complies with the appropriate specifications. A section was cut from Sample 3 for metallographic examination of the chrome plate and base metal structure. Figure 41 shows the chrome plate structure on the left side in the photomicrograph, and the faint black lines in this all white region are interpreted as grain boundaries. Locations 1, 2, 3, and 4 in this photomicrograph are typical microcracks which result from the chrome-plating process. The highly deformed "waviness" along flute tips mentioned previously is evident in this photomicrograph (far left side) by the ragged surface of the chrome plate. The interfacial area appears well bonded; i.e., no gaps or local areas of breakdown between chrome plate and base metal. The tempered martensite structure of the base metal is satisfactory, indicating proper heat treatment, and it is low in nonmetallic inclusions as expected by the low P and S levels shown in Table XI.

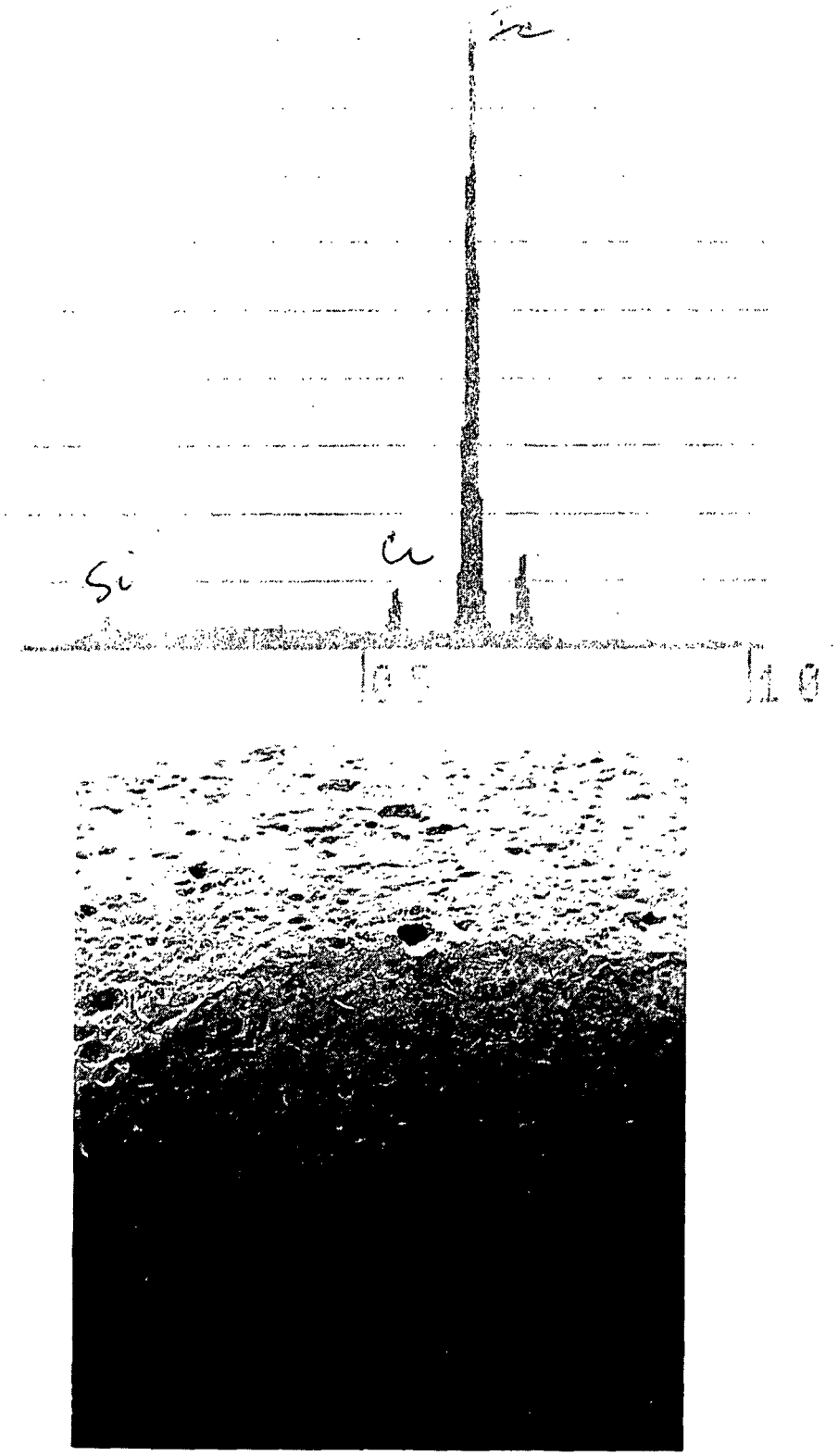

Figure 37. SEM Photograph (40X) and X-ray Spectra of the Flute Tip in Sample 3

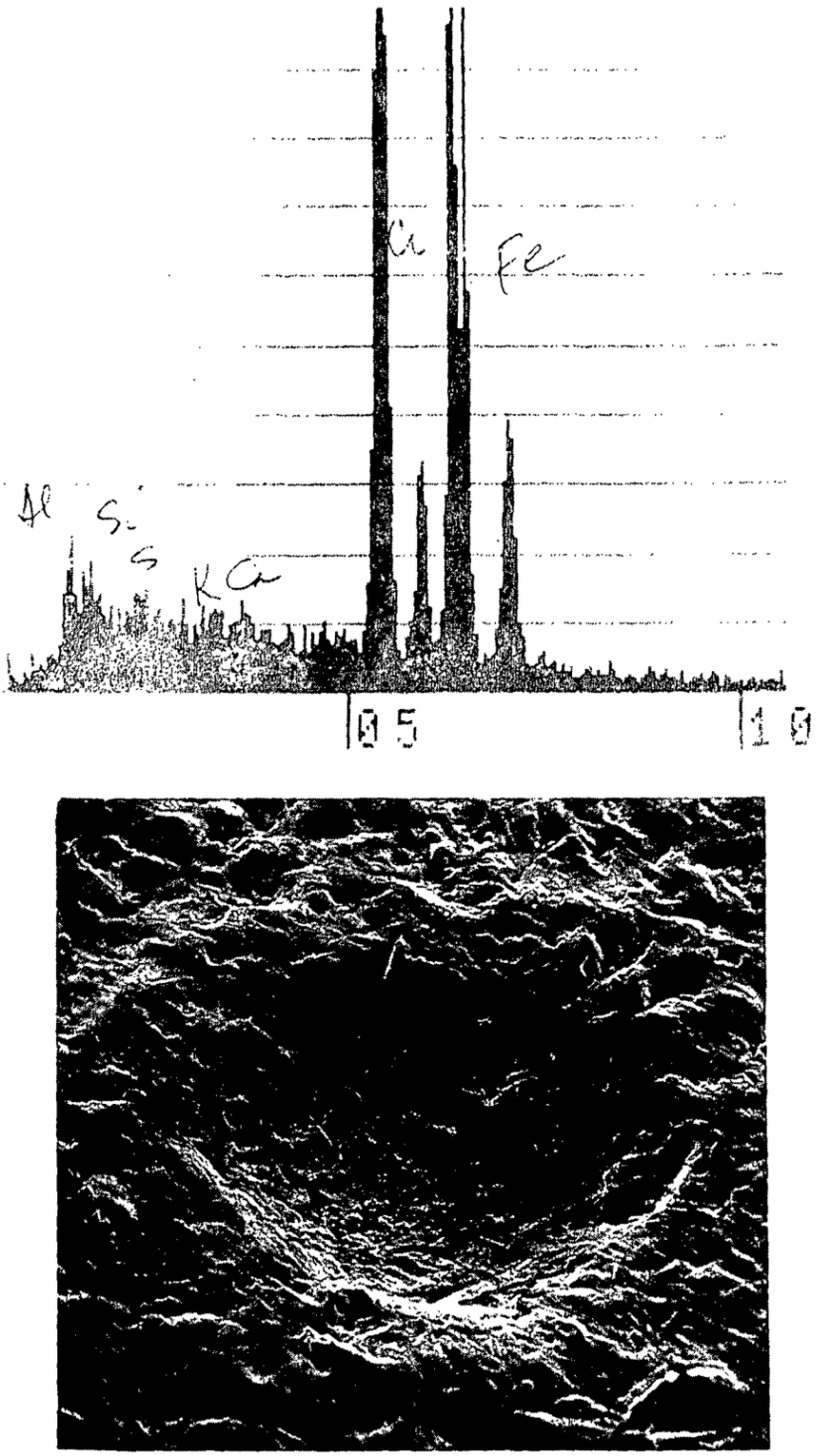

Figure 38. SEM Photograph (200X) and X-ray Spectra of a Local Region Typical to That Found Along the Side of the Flute in Sample 3

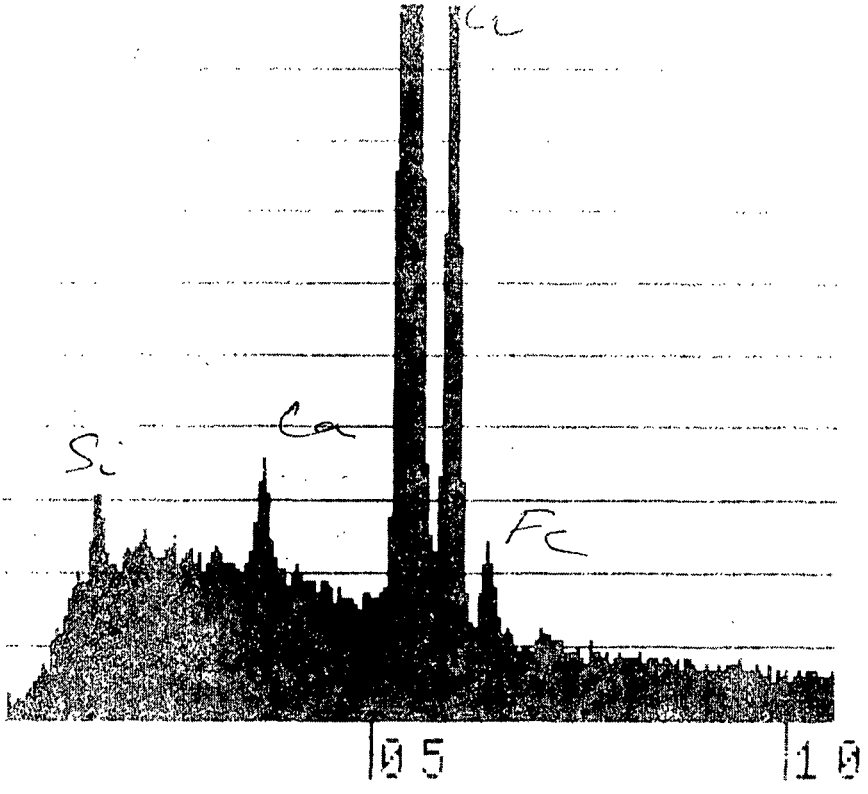

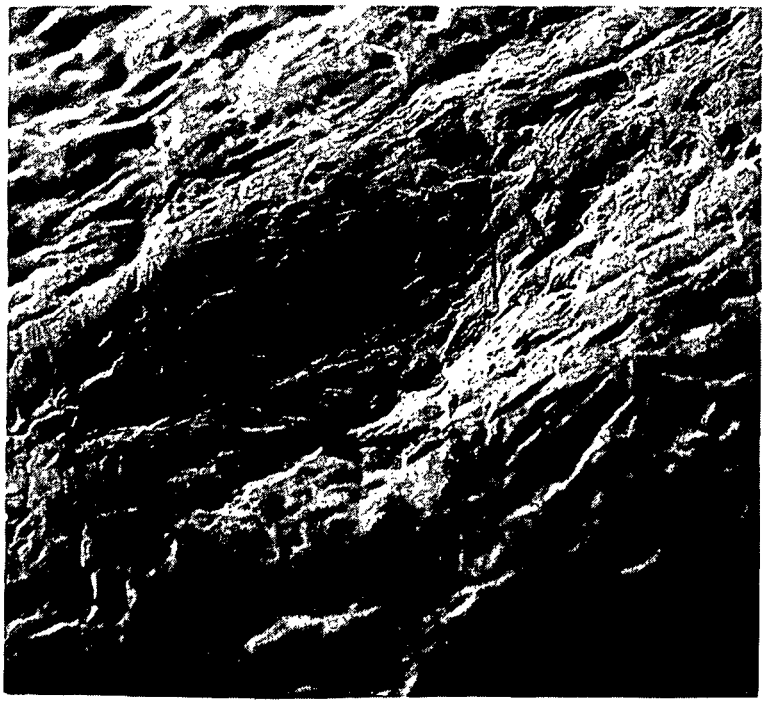

Figure 39. Same as Figure 19, Taken in a Different Area Along the Side of the Flute. Magnification 300X

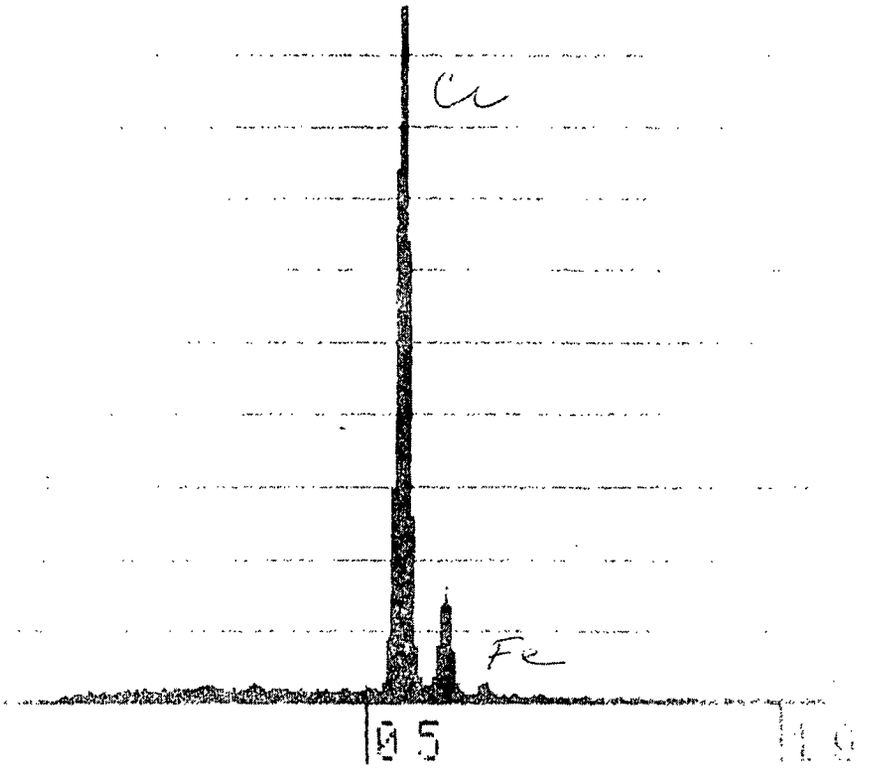

Figure 40. X-ray Spectra of Area Where Some Chrome Plate Remained on the Tip of the Flute Within the Working Width of the Roll

TABLE XI

CHEMICAL COMPOSITION AND HARDNESS OF CORRUGATING ROLL

Element	S.A.E. Specification	Analysis of Toll[a]	Hardness Specified	Hardness Measured[a]
			BASE METAL	
C	0.38 - 0.43	0.42	350-390 BHN	362-371 BHN
Mn	0.60 - 0.80	0.68	CHROME PLATE	
Sl	0.20 - 0.35	0.26	700 DPH	895-1007 DPH[b]
P	0.04 Max.	0.009		
S	0.04 Max.	0.008		
Ni	1.65 - 2.00	1.65		
Cr	0.70 - 0.90	0.72		
Mo	0.20 - 0.30	0.20		

[a] Analysis performed by Chas. C. Kawin Company Metallurgical Laboratories.
[b] Hardness measured by Knoop then converted to Vickers DPH.

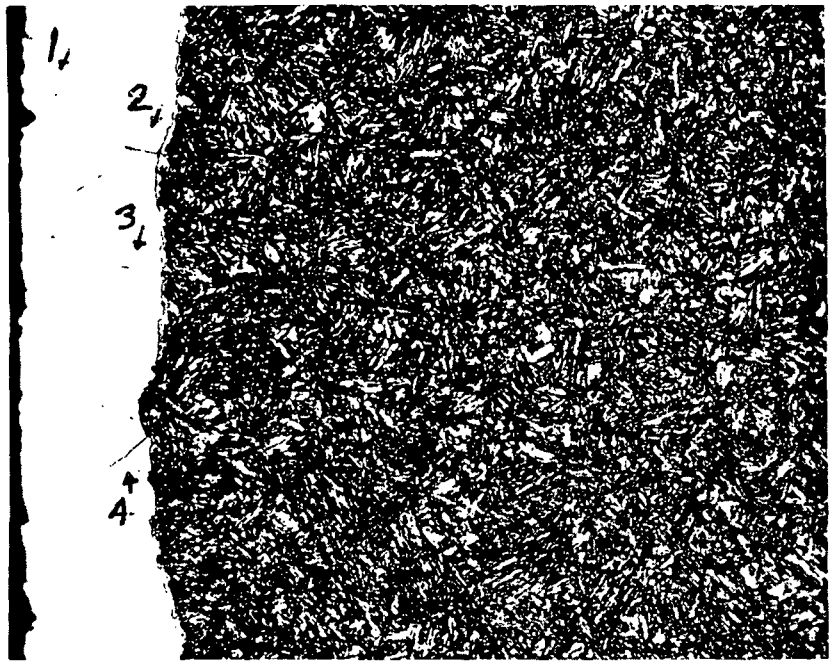

Figure 41. Section Through Plating Illustrating What Appears to be Good Quality and Adherence. The Base Metal Microstructure of Tempered Martensite Appears to be Normal with no Evidence of Excessive Inclusions or Defects

The chemistry of the feedwater used to generate steam and that of the water used on the rolls is shown in Table XII. Corrosion by general pitting from chloride attack in an aqueous system would not be expected on the base metal below a level of 100 ppm nor that of the chrome plate below 200-300 ppm chloride (20). Chloride ion contents of 76 and 20 ppm were noted for the soft water and steam, respectively.

The oil used to lubricate this roll was changed early in its service life from Gulf Oil's "Harmony 44" to "Security 39." The properties of these oils are shown in Table XIII. "Security 39," currently in service, was used during most of the service life of this roll because it provided better antisticking properties. It is a straight mineral oil without additives, and its lower viscosity at operating temperatures provides a lighter film coverage during operation. "Harmony 44"

contains corrosion inhibitors, chelating agents, and defoamers but it is higher in viscosity. Neither oil is resistant to breakdown and/or oxidation above 300°F (21).

TABLE XII

WATER ANALYSIS REPORT[a]

	Type or Source		
	Raw Water	Soft Water	Feed Water
Total hardness or $CaCO_3$, ppm	5 oz	Trace	1
Phenolphthalien Alkalinity as $CaCO_3$	0	0	8
Methyl Orange Alkalinity as $CaCO_3$	340	340	70
Chloride as Cl, ppm	80	70	20
pH	8.3	8.6	8.9
Calcium as $CaCO_3$, ppm			0.4
Magnesium as $CaCO_3$, ppm			0.6
Specific conductance Micromhos 25 C (corrected)	920	1075	325

[a]Furnished to the mill by Betz Laboratories.

A sample of the corrugating medium used on this roll was analyzed for ash content. The total ash content was 2.10% (2 hours at 900°C). The silicon content (reported as SiO_2) was 0.56%. Microscopic examination of the ash disclosed glass fibers approximately 15 microns in diameter and 1 millimeter in length. Traces of TiO_2 and clay were also observed in the ash but their abrasiveness is probably very small compared to the glass fibers.

TABLE XIII

TYPICAL PROPERTIES OF LUBRICATION OILS
USED ON CORRUGATING ROLLS[a]

Property	Oil Type	
	Security 39	Harmony 44
Gravity: °API	32.4	31.4
Viscosity, SUV: Sec.	105.5	150.2
100°F	105.5	150.2
210°F	39.8	43.3
Viscosity index	97	102
Flash, OC: °F	390	410
Fire, OC: °F	445	465
Pour: °F	+5	+5
Color, ASTM D1500	L0.5	L0.5
Carbon residue, rams: %	0.06	0.07
Neutralization value ASTM D974 Total acid no.	0.03	--

[a]Furnished by Gulf Oil Company, U.S.A.

CONCLUSIONS

The valley-tip areas of the flute are subject to high stress due to the sliding and rolling action that occurs during operation. The repetitive nature of this process leads to damage by surface fatigue or more appropriately corrosion fatigue at the surface. The initiation phase of corrosion fatigue is a combination of stress conditions (magnitude and direction as influenced by design geometry) and surface breakdown. Surface breakdown may be chemical (corrosion process), mechanical (cutting, scraping, etc.) or both. Once breakdown occurs, the stresses may produce

microscopic cracks which undermine small local regions at the surface. These regions may ultimately "pop-off" during continued operation and form pits (surface fatigue). Alternatively, stress conditions may propagate the crack through the entire cross section (fatigue fracture). Since cracks, pits and spalled areas in the chrome plate were observed in the nonworking width and "perforated craters (enlarged pits)" in the working width, surface fatigue is definitely one of the operative processes causing roll damage.

In addition, if the load-carrying capacity of the lubricant is inadequate, "scoring" occurs. Scoring entails the rapid removal of metal caused by tearing out small contacting particles bonded together as a result of metal to metal contact (22). This could be a dominant damage process during "running-in" of new rolls, i.e., operating in the absence of corrugating medium.

The corrugating medium is an effective agent toward fatigue crack initiation by its abrasive action on the roll contact surfaces. Crack propagation is facilitated by residual stresses from machining and chrome plating as well as the operating stresses. The formation of pits which develop into "craters" at a later time indicates the highly localized nature of the stress conditions, preferring crack re-entry at the surface rather than through section crack penetration.

This investigation did not show corrosion as a major cause of roll damage. Corrosion processes undoubtedly aid the initiation process of surface fatigue cracks because once the chrome plate is removed and base metal exposed, electrochemical action occurs between the small anodic base metal and large cathodic chrome plated areas. Any water residue remaining on the rolls after cleaning or as a contaminant in the lubricant would enhance this corrosive contribution.

It was difficult to characterize the original condition of the metal, because no formal records of the initial surface properties or quality of chrome plate of this roll is available. The metallurgical properties of the base metal were correct as specified and considered adequate for this application. The evaluation of surface residual stress and surface roughness prior to corrugating service are critical factors in roll life and these should be analyzed in future studies.

Glass fibers in the medium, relatively high temperature, and low load-bearing capacity of the lubricant are all damaging environmental influences. The reported pH of 7.5 to 8.0 for the corrugating medium is within an acceptable range for a chrome plate from a corrosion standpoint (19). However, if excessive oxidation of the oil occurs at the high operating temperature, an acid condition results – chrome plate is unstable at or below 4.5 pH. The particle size of the glass fibers contained in the medium may also be critical. In other studies of chrome plate wear resistance, the most damaging particle size of a dust abrasive in the lubricant was in the range of 15 to 20 microns (23).

In summary, this analysis indicates that reduced roll life is associated with surface fatigue. Initiation of this damaging process occurs by "scoring" from metal to metal contact and by abrasion from the medium during corrugating. Also microcracks are present and virtually impossible to avoid in the original chrome plating operation. Localized stresses propagate the cracks initiated and pits form and grow into "craters." Corrosion accelerates both initiation and propagation stages. The corrosion process is galvanic and it is promoted by the presence of moisture, high temperature and the oxidizing tendencies of the oil. The first region to suffer severe corrosion damage is the valley of the flute because chrome plate is very thin in these areas.

RECOMMENDATIONS

There are some possible corrective measures that deserve attention. These are as follows:

1. Inspection: The inspection of new rolls should include visual examination (5X) followed by $CuSO_4$ at points of damage. Dimensional checks to assure proper plate thickness should be accomplished by micrometer measurements. After installation and "running-in" of new rolls as well as at fixed intervals of corrugating time, these same measurements should be taken. Extent of damage, wear rate, and all other observations should be recorded with respect to time and location.

2. Based on the data in (1) above, the rolls should be removed for re-chrome plating at a suitable time when proper roll dimensions can be restored by this process. This can be done 2 or 3 times within the service life of a given set of rolls and represents a considerable savings over direct replacement from extended wear. Repair should be in accordance to ASTM B177.

3. The manufacturer should furnish the final hardness of chrome plate on new rolls. The hardness should not be lower than 700 Vickers or 600 if heat-treated. In addition, the mill inspection should include some type of hardness check. Scratch hardness measurements have been effectively correlated to wear on printing plate operations.

4. The manufacturer should furnish surface roughness measurements of new rolls as machined and chrome plated. The surface finish specified is RMS32-63. A measurable difference in wear can be expected with only 30% deviation from specification.

5. The removal of glass fibers or other contaminants from the medium could be accomplished by an improved cleaning system. Although the initial investment may be costly, the increase in roll life as well as all other components which handle this medium may justify it in the long term.

6. Lubrication: New rolls should be lubricated with an oil containing antiscruffing agents during the initial "running-in" period where there is metal to metal contact between upper and lower roll. During the corrugating process a lower viscosity oil is required for antisticking qualities but this oil should also provide wear protection and resist oxidation. Gulf Oil Co., U.S.A., has been contacted in this regard, and their representatives can make suitable recommendations concerning alternatives.

Lubrication control is also important. The lubricant should be applied in a continuous stream or mist, in measured amounts or intervals, and by suitable machine controls, e.g., flow rate sensors, etc.

7. Contamination and Cleaning: The chief sources of contamination are moisture, air borne dust, dirt or grit, and carryover products from adjacent machine components. Careful attention to eliminate these contaminants is the only reasonable preventative measure in this case. Nonabrasive cleaning agents free of acid constituents are a necessity to avoid roll surface damage. In addition, all moisture must be removed after cleaning, followed immediately by ample lubrication.

In the event that the above procedures are not sufficient in prolonging roll life, several alternative measures are considered important. These are as follows:

1. Improve surface finish by specifying at least 30% reduction in RMS surface roughness. This may be accomplished by additional final machining, via grinding, honing or lapping. It would correspond to 10 to 20 final RMS finish.

2. If chrome plate thickness can be increased without loss of adherence, via microcracks, an increase to 5 mils on the tip and 2.5 to 3 mils in the valley may be beneficial.

3. Shot peen the roll surface prior to final machining to reduce residual stress and improve fatigue strength, if practical.

4. Minimize embrittling effects of cleaning and plating by heat-treating rolls per AMS2406E, i.e., heating for not less than two hours at 300-500°F. This will remove the hydrogen inherent in the plating as well as provide additional stress-relief and improve resistance to cracking. The heat treatment will decrease the final hardness of both chrome plate and base metal but the wear resistance would improve because the chrome plate will be less brittle (24).

5. Alternate materials of construction should also be considered in the manufacture of corrugating rolls. This will be an expensive alternative and it would require extensive testing under actual process conditions. Possible candidate materials for this application are the Type 440 stainless steels, Haynes Stellite alloys 6B, 6K or No. 25, and suitable S-series tool steels. These materials can be hardened (>50Rc) and machined to the same surface finish requirements as presently specified or as recommended, to even lower RMS finish. One great advantage in the adoption of such materials is the elimination of plating which has poor resistance to wear by surface fatigue as shown in this report and as reported by others (25).

ACKNOWLEDGMENTS

The author expresses thanks to those mills who participated in these failure analyses. Acknowledgment is also extended to the Institute's Analytical and Photography Departments and the Machine Shop for their assistance.

LITERATURE CITED

1. Bowden, F. P., et al., Proceedings of the Royal Society, Series A, Vol. 263, 1961. 433-50.

2. Bowden, F. P., et al., Proceedings of the Royal Society, Series A, Vol. 282, 1964. p. 331-52.

3. Canabelis, R., Journal of Basic Engineering TASME, Series D, Vol. 90, 1968. p. 355-67.

4. Roetheli, B. E. and Brown, R. H., Ind. Eng. Chem., Vol. 23, 1931. p. 1010.

5. Russel, R. P., et al., Ind. Eng. Chem., Vol. 19, 1927. p. 65.

6. ASTM, STP 567, "Erosion, Wear and Interface with Corrosion," ASTM, Philadelphia, PA, 1975.

7. Copson, H. R., "Effects of Velocity on Corrosion," Corrosion 16(2):86-92t (1962).

8. Copson, H. R., "Effects of Velocity on Corrosion by Water," Ind. Eng. Chem., Vol. 44, 1952. p. 1745.

9. ASTM, STP 446, "Evaluation of Wear Testing," ASTM, Philadelphia, PA, 1969.

10. Fontana, M. G. and Greene, N. D., Corrosion Engineering, McGraw-Hill, 1967.

11. Metals Handbook, Properties and Selection of Metals, Vol. 1, 8th Edition, American Society for Metals, 1961.

12. Henthorne, M., "Stress Corrosion Cracking of Metals," Process Industries Corrosion, NACE, 1975. p. 123.

13. Klinge, L. N., et al., Chemical Cleaning of Equipment in Refiners and Petrochemical Plants, Corrosion, Vol. 16, 1959. p. 97-106.

14. Loucks, C. M., "Some Problems Associated with Contact Chemical Cleaning," Corrosion, Vol. 16, 1959. p. 18-26.

15. Gleekman, L. W., "Internal Cleaning of Plant Piping In-Place," Corrosion, Vol. 16, 1959. p. 15-26t.

16. Connick, B. J., "Field Test to Determine the Effectiveness of Inhibitor in Hydrochloric Acid," presented at N.A.C.E. Corrosion Conf., March 22-26, 1976. Preprint available from N.A.C.E.

17. Rydholm, S. A., Pulping Processes, Interscience Publishers, New York, 1965. p. 792.

18. Jones, R. L., et al., "The Potentiostatic Passivation of Mild Steel in 300°C NaOH Solutions," Corrosion, Vol. 26, No. 10, October, 1970. p. 399.

19. Jensen, W. L., "Failure of Mechanical Fasteners," Metals Handbook, Vol. 10, 8th Edition, 1975. p. 470-87.

20. Pourbaix, M., Atlas of Electrochemical Equilibria in Aqueous Solutions. Pergamon Press, London. 1966.

21. Kendrick, D. F., Gulf Oil — Houston, Private communication.

22. Metals Handbook, Vol. 1, "Properties and Selection of Metals," 8th edition, ASM, p. 511-24.

23. Metals Handbook, Vol. 10, "Failure Analysis and Prevention," 8th Edition, ASM, 1975. p. 251.

24. ASM Handbook, 1936 edition, American Society for Metals, p. 1098.

25. Poirier, C. C., "Why Anilox Rolls Fail," Spring Corrugated Containers Conference, June 4-6, 1974. p. 61.

THE INSTITUTE OF PAPER CHEMISTRY

D. F. Bowers
Research Associate
Assistant Professor

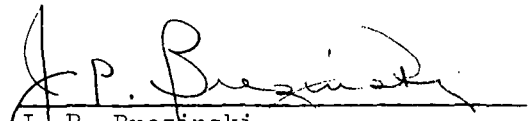

J. P. Brezinski
Director
Division of Materials
Engineering & Processes